BNWL-1381-2
UC-80

[redacted]

REACTOR PHYSICS QUARTERLY REPORT
APRIL, MAY, JUNE 1970

August 1970

[redacted]

AEC RESEARCH &
DEVELOPMENT REPORT

BNWL-1381-2

BATTELLE NORTHWEST
BATTELLE MEMORIAL INSTITUTE PACIFIC NORTHWEST LABORATORIES
BATTELLE BOULEVARD, P. O. BOX 999, RICHLAND, WASHINGTON 99352

LEGAL NOTICE

PACIFIC NORTHWEST LABORATORY
RICHLAND, WASHINGTON
operated by
BATTELLE MEMORIAL INSTITUTE
for the
UNITED STATES ATOMIC ENERGY COMMISSION UNDER CONTRACT AT(45-1)-1830

AEC-RL RICHLAND, WASH

BNWL-1381-2
UC-80,
Reactor Technology

REACTOR PHYSICS QUARTERLY REPORT
APRIL, MAY, JUNE 1970

By

The Staff of
Reactor Physics Department
L. C. Schmid, Manager
Physics Research Department
E. D. Clayton, Manager

and

Reactor Physics and Operations
of the FFTF
R. E. Heineman, Manager

August 1970

BATTELLE MEMORIAL INSTITUTE
PACIFIC NORTHWEST LABORATORIES
RICHLAND, WASHINGTON 99352

Printed in the United States of America
Available from
Clearinghouse for Federal Scientific and Technical Information
National Bureau of Standards, U.S. Department of Commerce
Springfield, Virginia 22151
Price: Printed Copy $3.00; Microfiche $0.65

REACTOR PHYSICS QUARTERLY REPORT
APRIL, MAY JUNE 1970

FOREWORD

The objective of the Reactor Physics Quarterly Report is to inform the scientific community in a timely manner of the technical progress made on the many phases of reactor physics work within the laboratory. The report contains brief technical discussions of accomplishments in all areas where significant progress has been made during the quarter. The results presented herein should be considered preliminary, and do not constitute final publication of the work. A list of publications and papers issued during the last quarter is included in the report. Anyone desiring additional information concerning the work reported herein is encouraged to contact the author directly.

PREVIOUS REPORTS IN THIS SERIES

HW-42182	October, November, December	1955
HW-43441	January, February, March	1956
HW-44525	April, May, June	1956
HW-47012	July, August, September	1956
HW-48893	October, November, December	1956
HW-50598	January, February, March	1957
HW-51983	April, May, June	1957
HW-53492	July, August, September	1957
HW-54591	October, November, December	1957
HW-55879	January, February, March	1958
HW-56919	April, May, June	1958
HW-57861	July, August, September	1958
HW-59126	October, November, December	1958
HW-60220	January, February, March	1959
HW-61181	April, May, June	1959
HW-62727	July, August, September	1959
HW-63576	October, November, December	1959
HW-64866	January, February, March	1960
HW-66215	April, May, June	1960
HW-67219	July, August, September	1960
HW-68389	October, November, December	1960
HW-69475	January, February, March	1961
HW-70716	April, May, June	1961
HW-71747	July, August, September	1961
HW-72586	October, November, December	1961
HW-73116	January, February, March	1962
HW-74190	April, May, June	1962
HW-75228	July, August, September	1962
HW-76128	October, November, December	1962
HW-77311	January, February, March	1963
HW-77871	April, May, June	1963
HW-79054	July, August, September	1963
HW-80020	October, November, December	1963
HW-81659	January, February, March	1964
HW-83187	April, May, June	1964
HW-84369	July, August, September	1964
HW-84608	October, November, December	1964
BNWL-95	January, February, March	1965
BNWL-149	April, May, June	1965
BNWL-193	July, August, September	1965
BNWL-222	October, November, December	1965
BNWL-284	January, February, March	1966
BNWL-315	April, May, June	1966
BNWL-340	July, August, September	1966
BNWL-400	October, November, December	1966
BNWL-472	January, February, March	1967
BNWL-534	April, May, June	1967

BNWL-634	July, August, September	1967
BNWL-685	October, November, December	1967
BNWL-775	January, February, March	1968
BNWL-887	April, May, June	1968
BNWL-921	July, August, September	1968
BNWL-985	October, November, December	1968
BNWL-1053	January, February, March	1969
BNWL-1150	April, May, June	1969
BNWL-1240	July, August, September	1969
BNWL-1304	October, November, December	1969
BNWL-1381-1	January, February, March	1970

CONTENTS

REACTOR PHYSICS QUARTERLY REPORT
April, May, June 1970

1.0 SUMMARY

THERMAL REACTORS

A detailed theoretical analysis is being made of the PRCF critical experiments conducted in the cooperative USAEC-CNEN program. Theoretical methods and calculational techniques are being evaluated by comparing calculated and measured reactivities and power distributions. In general, values of k_{eff} predicted via calculation are larger than measured values. Systematic differences are noted between calculated and measured power distributions. A simple modification in calculational technique significantly improves the power distribution correlation for the twelve configurations analyzed.

A new version of the nonlinear least-squares fitting program LEARN, called LEARN-I-C, has been written. The new version increases both reliability and speed in the solution of difficult problems.

Critical experiments were completed in the PRCF in an H_2O moderated lattice (1.06 in. square pitch) of UO_2-4 wt% PuO_2 fuel rods.

The radiochemical and mass spectrometric analysis of fuel samples taken from the PRTR Batch Core has been completed.

Gulf General Atomic, Inc., has completed the reanalysis of the plutonium lattice space dependent spectral measurements. A report (GA-10116) on the results of this research is being issued.

Subcritical measurements of critical numbers of rods for Al-Pu-H_2O and UO_2-PuO_2-H_2O systems made in the CAF are completed.

Interpretation of experimental data has been completed for the determination of k_∞ for a uniform lattice of 0.5-in. diameter UO_2-2.0 wt% PuO_2 rods at 1.0-in. square pitch in light water. The discrepancy between theoretical prediction and the value for k_∞ inferred from PCTR measurements, apparent in the preliminary analysis, has been resolved by a detailed re-evaluation of the experimental data. The previous discrepancy resulted from an accumulation of several small systematic errors which had been either neglected or improperly evaluated.

The following computer codes have been documented and released to the Argonne Code Center.

- BRT-I: Battelle-Revised-THERMOS-I
- BMC-I: The Battelle Monte Carlo Code
- HRG 3: A code for Calculating the Slowing-Down Spectrum in the P1 or B1 Approximation
- DBUFIT-I: A Least Squares Analysis Code for Nuclear Burnup Data.

An abstract of each of these codes can be found in Section 2.0.

Values of $k_\infty(T)$ for a ThO_2-$^{235}UC_2$-C HTGR lattice have been obtained from experiments in HTLTR at temperatures up to 1000 °C. The results are compared with values of $k_\infty(T)$ for the same lattice obtained from calculation. The measured change in k_∞ between 20 °C and 1000 °C is slightly larger than the calculated change, but the agreement is generally good.

Values of the overall temperature coefficient of reactivity for HTLTR as a function of temperature, measured during the second HTGR experiment (ThO_2-$^{233}UO_2$-0), were significantly different from the values calculated using the 2DB model of HTLTR. The large discrepancies preclude the use of the present model for predicting the change in HTLTR excess reactivity throughout an experiment to 1000 °C and loadings will have to be established in an empirical way until the causes of the discrepancies can be identified and removed.

A highly stable control system has been developed for controlling the pressure of the nitrogen atmosphere inside HTLTR. A fused quartz pressure gage has been interfaced with the PDP-7 Process Control Computer and special software programs have been developed which, in combination, control the reactor atmosphere pressure to within ±0.01 Torr of a preselected set point automatically. This precise control of the nitrogen pressure reduces or eliminates the need for corrections to reactivity data due to variations in pressure between or during measurements.

A computer program has been developed to calculate the temperature distribution in the plates of an HTLTR vertical safety rod as a function of time after insertion from a 20 °C environment into a 1000 °C environment. The program has been used, together with subsequent stress analyses, to confirm the cause of the recent VSR failure and to evaluate potential new VSR designs.

FAST REACTORS

A small UA1 fast core was installed in the center of the PCTR fast neutron cavity. Measured reactivity worths of the central cell and a standard absorber were analyzed to determine k_∞' for the fast core. Agreement between experiment and calculations builds confidence in the method. Very accurate measurements can be made of k_∞' for fast reactor cores having low leakage.

2.0 THERMAL REACTORS

CALCULATIONS OF POWER DISTRIBUTIONS AND REACTIVITIES

V. O. Uotinen, G. L. Gelhaus, U. P. Jenquin and C. R. Gordon

Introduction

A detailed analysis is in progress of the critical experiments conducted in the PRCF under a cooperative program[1] between the USAEC and the Italian CNEN. The purpose of this analysis is to evaluate calculational methods and models by comparing calculated power distributions and reactivities with those measured in the USAEC-CNEN program. The experimental program comprised a large number of lattice configurations using 2.35 wt% enriched UO_2 rods and PuO_2-UO_2 rods of several enrichments. The configurations ranged from simple uniform lattice arrays to arrays which simulated boiling water reactor fuel bundles with rods of lower enrichments on the edges and corners to reduce power peaking.

The analysis thus far has been applied to arrays in which a single type of fuel rod was used. This study comprises a total of 12 loadings, six configurations for each of two fuel types, 2.35 wt% enriched UO_2 and 2 wt% PuO_2-UO_2 (8% ^{240}Pu) rods. The six configurations were (1) a regular uniform loading of rods; (2) the same loading but with a water hole in the center (i.e., the central fuel rod was removed); (3) water slab (a row of fuel rods removed); (4) water cross; (5) a 7 × 7 rod array surrounded by water slots; (6) a similar 9 × 9 rod array.

In these twelve experiments, spatial power distributions were measured by gamma-scanning selected fuel rods. The k_{eff} for an infinitely-reflected array was also determined for each case. The main interest in the power distribution measurements was in the rod-to-rod distribution, expecially the effects of water slots on the power peaking.

The series of experiments, ranging from the simplest (regular) array to one simulating a 7 × 7 or 9 × 9 bundle, provides a systematic test for the evaluation of calculational methods.

Calculations

In the analysis of H_2O-moderated and reflected experiments (especially clean critical experiments) one generally assumes the reactor is composed of two regions: core and reflector. Few-group cross sections are calculated, assuming that an infinite medium spectrum applies in each region. The few-group cross sections are then used in a diffusion theory calculation of k_{eff}.

In an earlier study[2] it was pointed out that such a two-region, infinite medium model generally does not predict the power distribution well, although it may yield a satisfactory value for k_{eff}. In general, this method shows a pronounced trend, such that if the power distribution is normalized at the center of the core, the power near the core-reflector interface is consistently under-estimated. A simple modification, which resulted in considerably improved correlations, was reported in Reference 2. This simple modification consisted in introducing an extra reflector region (one lattice unit thick, adjacent to the core) which is represented by cross sections averaged over a spectrum characteristic of the core.

The multigroup transport theory codes HRG and Battelle-Revised - THERMOS were used to generate four-group cross sections for core and reflector regions. These cross sections were used in the two-dimensional diffusion theory code 2DB in an x-y calculation of power distributions and k_{eff}.

Four mesh points per cell were used in the 2DB calculations. This mesh description was carried out two lattice units

into the reflector; then the mesh points were more widely spaced. An axial buckling of 8.9 m^{-2} was used consistently.

In our current analysis we have compared three variations of our calculational model:

Model 1. The usual two-region, infinite-medium model (described in previous section);

Model 2. A simple modification consisting of an additional reflector region whose cross sections are obtained from cell calculations performed for the core (described in the previous section). In this model all water gaps also contained these modified reflector cross sections.

Model 3. A more detailed representation of the differences in spectrum in successive rows of fuel and water. This was accomplished with THERMOS calculations in slab geometry, with appropriate homogenized regions of core, reflector and gaps; editing was done over the proper spatial points to obtain average cross sections for each "row" of fuel and water. For analysis of the UO_2 loadings, five sets of core cross sections were used to represent fuel rods in various locations, and four sets of cross sections were used to represent water. For analysis of the UO_2-PuO_2 loadings, three sets of core cross sections and three sets of water cross sections were used.

Results

Power Distributions

Power distributions calculated using the three models described above were compared with measured distributions.

The trend that is so evident in the regular lattices when using Model 1 (i.e., calculated power consistently underestimated near core-reflector boundary) was significantly reduced when the modified models were used. The simple

modification used in Model 2 gives a better correlation than the more refined modification used in Model 3. This is evident especially in the case of the mixed oxide loading.

The lattice position that one chooses for a normalization point is rather arbitrary, yet this choice can affect the trends that one sees as well as the overall goodness or badness of the correlation. The center of the core is one likely normalization point. However, if this point is chosen, then one is basing his whole correlation on the accuracy of that one measurement (since there is only one rod in the center). A better choice might be a location away from the center and also away from water boundaries, a location which would permit four or eight symmetrical rods to be measured, the average of these measurements then providing a more reliable normalization point. However, multiple symmetrical rods were not measured in every case. Furthermore, no matter what point one chooses, there are always nonuniformities in the fuel rods, in the lattice plates, and bowing of fuel rods, etc., which introduce unknown errors into the normalization.

To eliminate this arbitrariness, and to provide a meaningful and consistent criterion for comparison of methods, we chose to represent the goodness of each correlation by a standard deviation, σ, defined by[1]

$$\sigma = \sqrt{\sum_{i}^{N} (\bar{\delta} - \delta_i)^2/(N - 1)}$$

where N is the number of rods measured,

$$\delta_i = \frac{P_{calc} - P_{meas}}{P_{meas}} \text{ for the } i^{th} \text{ rod,}$$

and $$\bar{\delta} = \sum_{i}^{N} \delta_i/N.$$

The definition of σ implies an "effective" normalization such that the average fractional deviation, δ, is zero. This definition thus makes σ independent of the particular choice of normalization, and provides us a meaningful, consistent measure for purposes of comparing methods.

The σ's for the various cases are given in Table 2.1. We can make the following general observations:

- In every case σ was significantly reduced when modifications were made to the simple two-region, infinite medium model (Model 1).
- In most cases, Model 2 gives the best correlation.

The significant improvement, and the goodness of the correlations obtained with the simple modification (Model 2), as well as its simplicity, make this model attractive for calculating power distributions in H_2O cores.

Calculation of k_{eff}

The modifications that were introduced to the two-region, infinite-medium model to improve power distribution correlations resulted in increases in calculated values of k_{eff}. This is consistent with comparisons between transport and diffusion theory results[3] which indicate that transport theory gives higher values of k_{eff}. That is, when one represents the core-reflector boundary with a better model (be it transport theory or a modification to diffusion theory) this results in higher values of k_{eff}. The calculated values of k_{eff} are listed in Table 2.2.

For the UO_2 loadings, the k_{eff} calculated using Model 1 were consistently low, with discrepancies ranging from 0.24 to 1.7%. Best agreement between measured and calculated k_{eff} values was obtained using Model 2, with discrepancies ranging from +0.34% to -0.17%. Model 3 gave consistently high values of k_{eff} (by 1.0% to 1.7%).

TABLE 2.1. Standard Deviation (%) in Power Distributions

	UO_2			PuO_2-UO_2		
	Model 1	Model 2	Model 3	Model 1	Model 2	Model 3
Regular	2.09	1.18	1.05	3.37	1.86	2.17
H_2O-hole	1.48	0.98	1.14	2.48	1.78	-
H_2O Slab	1.95	1.48	1.56	1.60	1.38	1.13
H_2O Cross	1.57	1.37	1.21	2.13	1.40	-
7 x 7	1.96	1.72	2.16	2.26	1.69	1.78
9 x 9	2.91	2.67	3.12	2.29	1.90	-

TABLE 2.2. Values of k_{eff}

	UO_2				PuO_2-UO_2			
	Exp.	Model 1	Model 2	Model 3	Exp.	Model 1	Model 2	Model 3
Regular	1.0032	1.0008	1.0051	1.0164	1.0006	0.9960	1.0080	1.0009
H_2O Hole	1.0025	1.0000	1.0046	1.0161	1.0020	0.9973	1.0096	-
H_2O Slab	1.0018	0.9957	1.0044	1.0162	1.0068	0.9982	1.0182	1.0063
H_2O Cross	1.0010	0.9924	1.0039	1.0161	1.0054	0.9956	1.0231	-
7 x 7	1.0010	0.9888	1.0044	1.0175	1.0038	0.9867	1.0220	1.0007
9 x 9	1.0027	0.9858	1.0010	1.0133	1.0078	0.9928	1.0245	-

For the PuO_2-UO_2 loadings, the k_{eff} calculated using Model 1 were consistently low, with the discrepancies ranging from 0.5 to 1.7%. The k_{eff} calculated using Model 2 were consistently high, with discrepancies ranging from 0.7 to 1.8%; Model 3 gave the closest agreement with measured k_{eff} values.

Conclusions

The simple modification incorporated in Model 2 of our analysis significantly improved power distribution correlations for the twelve configurations that were analyzed.

This improvement, together with the simplicity of this method, makes this method attractive for calculating power distributions in H_2O cores. The simplicity of the model comes about because cross sections for the modified water regions (water gaps and the reflector adjacent to the core) are obtained directly from cell calculations for the core. No additional calculations are necessary.

The method will next be used to calculate power distributions in more complex loadings which contain fuel rods of several enrichments.

References

1. *P. Loizzo, et al. Experimental and Calculated Results for UO_2 and UO_2-PuO_2 Fueled H_2O-Moderated Loadings, To be published, Battelle-Northwest.*

2. *V. O. Uotinen, G. L. Gelhaus, S. R. Dwivedi. "Analytical Correlations of Measured Power Distributions," Plutonium Utilization Program Technical Activities Report, March, April, May 1969, BNWL-1106, Battelle-Northwest. July 1969.*

3. *S. R. Dwivedi. "Multiplication Dependence on Energy and Angular Detail in Transport Theory Calculations," Plutonium Utilization Program Technical Activities Quarterly Report, June, July, August 1969, BNWL-1224, Battelle-Northwest October 1969.*

NONLINEAR LEAST-SQUARES DATA ANALYSES

D. A. Kottwitz

A new version of the nonlinear least-squares fitting program LEARN,[1] called LEARN-I-C, has been written and is ready for general use. This program supercedes versions LEARN-I-A[2] and LEARN-I-B.[3] This version includes modifications which increase both reliability and speed for difficult problems. In addition, three new options concerning the plotting of graphical output on the CALCOMP plotter are available to the user at execution time:

1) Optional number of times the graph is traced,
2) Optional distance between the initial pen position and the edge of the paper,
3) Optional spacing between successive origins in case of multiple plots during a single run.

References

1. *G. D. Seybold. User's AID: Programs LEARN and LIKELY, BNWL-1057. Battelle-Northwest. May 1969.*
2. *D. A. Kottwitz. "Constraints in Nonlinear Least-Squares Program LEARN," Reactor Physics Quarterly Report, July, August, September, 1969, BNWL-1240. Battelle-Northwest. November 1969.*
3. *D. A. Kottwitz. "Nonlinear Least-Squares Data Analyses," Plutonium Utilization Program Technical Activities Quarterly Report, September, October and November 1969. Battelle-Northwest. January 1970.*

CRITICAL EXPERIMENTS IN UO_2-4 wt% PuO_2 FUELED-H_2O MODERATED ASSEMBLIES

W. P. Stinson

Critical experiments were conducted in the Plutonium Recycle Critical Facility (PRCF) to obtain data for verifying the accuracy of neutronic design methods. The fuel rods contained UO_2-4 wt% PuO_2 with 18% ^{240}Pu[1] and the moderator was H_2O.

The core consisted of the fuel (1/2 in. diameter rods) in a 1.06 in. square lattice pitch loaded to form a cylinder with a 36 in. height and a radius equivalent to 126 fuel rods when critical. The measurements conducted on this core were:

- Critical size
- Kinetic parameters (β/ℓ)
- Flux distributions
- Void coefficient
- Approach-to-critical.

Approach-to-critical data were taken as a check on the techniques used in similar type measurements made in the Critical Approach Facility (CAF). The critical loading inferred from the subcritical approach was 126.70 ± 0.04 rods which agrees well with the actual critical loading of 126.44 ± 0.07 rods.

The kinetics measurements were made by recording and analyzing the reactor noise. The preliminary value of β/ℓ obtained is 93 ± 2 sec^{-1}. The flux distribution was measured by scanning the fuel rods for fission product decay gamma rays. Empty thin-wall aluminum tubes were placed in interstitial positions in the central part of the core to obtain data from which the void coefficient can be determined. Analysis of the data is continuing to obtain final values.

Reference

1. *L. C. Schmid et al. "Fuel Description," Reactor Physics Data for the Utilization of Plutonium in Thermal Reactors, BNWL-801, p. A2. Battelle-Northwest. May 1968.*

BURNUP DATA FROM THE PRTR BATCH CORE EXPERIMENT

D. E. Christensen and R. P. Matsen

Fourteen rods of the PRTR Batch Core Experiment[1] were selected for destructive analysis. Thirty five samples were

cut from these fourteen rods. A gross gamma scan was made of each rod to measure the fission profile of the rod in order to select appropriate samples. Gamma ray spectra were then taken at the positions of the individual samples. The location and irradiation history of the samples are given in Table 2.3. The initial composition of the various plutonium fuel lots are shown in Table 2.4. Within an element, positions j, n, and r are from the 12-rod or exterior ring, positions c and f are from the 6-rod or middle ring, and position a is the center rod of the nineteen rod cluster. The location of each sample with respect to the top of the fuel (including the UO_2 pellet) is also indicated in Table 2.3.

The destructive analysis data have been processed through the data analysis code, ISODIL. Preliminary results indicates the maximum exposure is 9630 MWd/MTM for the sample from the exterior rod in Element 6063 which was located in the first ring of the core.

Additional analysis of the data will be made to derive ratios of effective cross sections. The isotopic data will be used in conjunction with the gamma ray spectral data in studies which seek to determine fuel burnup nondestructively. All the data will be used as a basis for verifying the accuracy of neutron design methods in predicting reactor burnup.

Reference

1. *J. R. Worden, W. L. Purcell and L. C. Schmid. Physics Experiment-High Power Density Core of the PRTR, BNWL-221, Battelle-Northwest. 1966.*

GULF GENERAL ATOMIC SPECTRAL DATA

The reanalysis of the plutonium lattice space dependent spectral measurements conducted by Gulf General Atomic, Inc.

TABLE 2.3. Batch Core Samples

Fuel Element No.	Position in Reactor (Ring)	Rod No.	Position in Element	Pu Fuel Lot	Irradiation Terminated on	Removal During	Sample	Position* in Rod, in.	Approximate Date that Samples Analysed	Exposure, MWd/MTM
6065	3	FS12	r	62-23	9-10-67	Interim Test 1	1	6.5	9-10-68	1540
							2A	10.4	9-10-68	1770
							3A	29.4	9-10-68	2900
							4	41.3	9-10-68	2490
							5	47.5	9-10-68	2140
6066	3	FS16	r	62-23	1-28-68	Interim Test 2	1	6.5	6-15-69	3360
							2	9.6	6-15-69	3960
							3	28.9	6-15-69	5970
							4	43.6	6-15-69	5290
							5	48.1	6-15-69	4650
		F079	c	62-22	1-28-68		1	6.5	6-15-69	2120
							2	10.4	6-15-69	2640
							3	30.9	6-15-69	3850
							5	47.3	6-15-69	3050
		FE77	a	62-23	1-28-68		1	6.5	6-15-69	1810
							3	30.3	6-15-69	3270
							5	47.6	6-15-69	2700

* *Length of Fuel = 58.675 ± 0.125 in. which includes 57.837 ± 0.125 in. of UO_2-PuO_2 and a UO_2 pellet on each end.*

TABLE 2.3 (contd)

Fuel Element No.	Position in Reactor (Ring)	Rod No.	Position on Element	Pu Fuel Lot	Irradiation Terminated on	Removal During	Sample	Position in Rod, in.	Approximate Date that Samples Analyzed	Exposure, MTd/MTM
6063	1	FS01	n	62-23	6-1-68	Interim Test 3	3	28.9	6-15-69	8920
6067	3	FS23	r	62-23	6-1-68		1	6.5	6-15-69	4520
							2	9.7	6-15-69	5340
							3	29.1	6-15-69	8050
							4	43.5	6-15-69	7250
							5	48.5	6-15-69	6590
6058	5	FS08	j	62-23	6-1-68		3	29.9	6-15-69	7130
6516	7	FR64	j	62-6	6-1-68		3	30.5	6-15-69	5800
6520	1	FR78	n	62-18	7-14-68	Interim Test 4 (Reactor Shutdown)	1	30.4	4-1-70	9630
6065	3	FS07	j	62-23	7-14-68		1	30.4	4-1-70	9180
		F017	c	62-22	7-14-68		2	10.0	4-1-70	3920
							3	30.4	4-1-70	5840
		FE74	a	62-23	7-14-68		2	10.0	4-1-70	3290
							3	30.4	4-1-70	4860
6519	7	FN86	f	62-18	7-14-68		1	7.8	4-1-70	1940
							2	30.4	4-1-70	3300
		FE69	a	62-10	7-14-68		1	7.8	4-1-70	1710
							2	30.4	4-1-70	2880

TABLE 2.4. Initial Composition of Plutonium Fuel Lots

Fuel Lot	^{238}Pu	^{239}Pu	^{240}Pu	^{241}Pu	^{242}Pu
62-23	0.026	90.526	8.229	1.139	0.080
62-22	0.016	91.119	8.085	0.739	0.041
62-6, 62-10, 62-18	Unknown	91.045	8.086	0.817	0.052

has been completed. A final report entitled Reanalysis of Plutonium Lattice Spectral Data, GA-10116, has been written and is being issued. The Introduction and Conclusions sections of this report are repeated here.

Introduction

"This report describes the research performed for Pacific Northwest Laboratory (PNL) through USAEC Contract AT(45-1)-1830 during the period November 1, 1969 through April 30, 1970. The research covers the reanalysis and documentation of the data measured at Gulf General Atomic for the U.S. Atomic Energy Commission under Contract AT(04-3)-167, Project Agreement No. 32. These data were time-of-flight thermal neutron spectra measured at various positions and at different temperatures in H_2O-moderated lattices of Pu-Al fuel. In this program significant distortions were found in the spectral data that were believed to be due to complex neutron emission time effects which could not be treated at the time with existing codes. In the program conducted for PNL, these effects have been corrected for as far as possible and the revised measured and calculated data have been listed for reference use.

"The experiments performed are described in detail in Reference 1; however, for the sake of completeness, a brief

description is given in Section 2 of this report. Section 3 describes the problems encountered in the experimental data and the treatment that has been given to them. We discuss the trends in the revised experimental data and their comparison to theory in Section 4. The measured and calculated values are listed in the appendices."

Conclusions

"From the present analysis of the thermal neutron spectra in Pu-Al lattices, several conclusions can be drawn:

1. A fairly good agreement (within 10%) exists between the calculated and the measured power distribution in the cell.
2. Relative temperature effects are well taken care of by the Haywood-II scattering kernel for H_2O.
3. Slowing down and thermalization processes are reasonably well understood and in the framework of the present analysis, no significant neutron emission time problems remain."

"However, this work leaves unanswered two questions:

1. The mechanism for the distinct shift of the 0.3 eV resonance flux dip towards low energies.
2. The lower effective temperature of the measured spectra with respect to calculations.

On the basis of the present information, it can be said that the second question casts some doubts about the ability of the Haywood kernel to describe accurately the energy exchanges taking place in strongly anisotropic situations. It is difficult to be definite on this point since it should be recalled that the calculations depend on various approximations concerning the description of the cell geometry and the neutron source and the angular representation of the neutron flux.

Finally, let us point out that aspects of the experiments which are not fully understood prevent evaluation of the quality of certain cross sections used in the computation, particularly those of ^{239}Pu."

Pu-H_2O LATTICE SUBCRITICAL EXPERIMENTS

J. H. Lauby

Experiments were conducted in the Critical Approach Facility (CAF) to measure the critical mass of some plutonium-fueled, H_2O-moderated lattices. These lattices were repeats of some of those in which measurements of the critical numbers of rods were made for Al-Pu-H_2O and UO_2-PuO_2-H_2O systems.[1] The UO_2-PuO_2 fueled lattices were "remeasured" to determine the effect of ^{241}Pu decay on the number of rods for critical.[2] The Al-Pu fueled lattices were remeasured to determine the combined critical mass effect of removing Lucite tubes which surrounded each fuel rod and ^{241}Pu decay. The reduction of the data collected in these experiments are completed, and the results are summarized in Table 2.5 with results obtained from the earlier measurements.[1] A destructive analysis of one of each of these fuel rods is also being made to determine isotopic compositions.

The new results for the Al-1.82 wt% fueled lattices show a decrease in the critical mass for the 0.75 and 0.85 lattices which are undermoderated and an increase in the critical mass for the 0.93 in. lattice which is over-moderated. Decay of ^{241}Pu would increase the critical number of rods for all lattices. Since the ^{241}Pu concentration originally in these rods was quite small the major perturbation is the removal of Lucite sleeves. If it is assumed that Lucite and H_2O are identical from a reactor physics standpoint, then the observed effects could be explained by assuming voids existed between the sleeves and the fuel rods. The new results for the

TABLE 2.5. Comparison of Measured Critical Masses

Fuel	Hexagonal Lattice Spacing, in.	Critical Number of Rods			
		New Values	Date, mo/yr[(a)]	Previous Values	Date, mo/yr[(a)]
Al-1.83 wt% Pu (5.58 wt% ^{240}Pu, 0.44 wt% ^{241}Pu)	0.75	541 ± 1	1/70	563 ± 1	1/62
	0.85	486 ± 2	12/69	494 ± 1	2/62
	0.93	560 ± 2	1/70	547[(b)]	--
Al-2.01 wt% Pu (16.46 wt% ^{240}Pu, 2.31 wt% ^{241}Pu)	0.75	861 ± 1	1/70	848 ± 1	9/63
	0.85	826 ± 1	2/70	786 ± 1	8/63
	0.93	1115 ± 5	1/70	1040 ± 2	1/66
UO_2-2 wt% PuO_2 (23.5 wt% ^{240}Pu, 4.08 wt% ^{241}Pu)	0.93	308 ± 1	1/70	288 ± 1	7/65
Uo_2-4 wt% PuO_2 (18.10 wt% ^{240}Pu, 5.08 wt% ^{241}Pu)	0.93	180 ± 1	4/70	179 ± 1	12/68

(a) Month and year in which experiment was conducted.

(b) Value interpolated from curve of Critical Number of Rods Versus H/Pu Atom Ratio

Al-2 wt% Pu fueled lattices show that the critical number of rods increased for all lattices. Therefore it appears that the ^{241}Pu decay is the major effect since it is expected that removing the Lucite sleeves would decrease the critical mass for the 0.75 and 0.85 in. lattices.

The new values for the UO_2-PuO_2 systems illustrate the effect of ^{241}Pu decay. A four and one-half year decay period leads to a 6.9% increase (i.e. 20 rods) in the critical number of rods for the UO_2-2 wt% PuO_2 lattices.

The results of this study show that ^{241}Pu decay has a non-negligible effect on criticality. Repeating these measurements a couple of years hence would provide additional valuable data on the time dependent reactivity effect of ^{241}Pu decay to ^{241}Am.

References

1. *L. C. Schmid, et al. Reactor Physics Data for the Utilization of Plutonium in Thermal Power Reactors, BNWL-801, Battelle-Northwest. May 28, 1969.*

2. *V. O. Uotinen. "The Effect of ^{241}Pu Decay on the Analysis of Plutonium Critical Experiments," submitted for publication in Nuc. Sci. and Eng., BNWL-SA-3157.*

INTERPRETATION OF k_∞ FOR WATER MODERATED UO_2-PuO_2 LATTICES

D. F. Newman and C. R. Gordon

Introduction

The development of a water tank in the Physical Constants Testing Reactor (PCTR)[1] during FY 1968 enabled the performance of light water moderated lattice experiments in the PCTR. Measurements of k_∞ and other neutronic parameters were obtained for a uniform lattice of 0.5-in. diameter UO_2-2.0 wt% PuO_2 (7.74 wt% ^{240}Pu) rods at 1.0-in. square pitch in light water.[2] Preliminary analysis of the experimental data indicated a 6% discrepancy between theoretical predictions and the

value for k_∞ inferred from PCTR measurements.[3] An extensive study of the theoretical models, analytical techniques, and experimental measurements used in the correlation was undertaken. The apparent discrepancy has been resolved by a detailed reevaluation of the experimental data.

Activation Foil Perturbation Corrections

Foil activation techniques are used in the determination of the relative reaction rates in all central cell constituents and the standard absorber (usually copper) inserted in the center of the PCTR. The presence of foil materials in the lattice perturbs the neutron flux in the vicinity of each foil, such that the induced activity is not truly representative of the flux in the surrounding unperturbed media.

Two-dimensional transport theory calculations in two energy groups were performed using DOTSN,[4] explicitly including foils in the lattice cell geometry used to measure activation rates. Thermal group constants were calculated using BATTELLE-REVISED-THERMOS Code;[5] epithermal group constants were calculated using the HRG[6] Code. Calculated two-group neutron flux perturbations in the foil regions of the R-Z geometry lattice cell were used to correct the measured subcadmium and epithermal activation rates to represent the two group activation rates in the unperturbed media.

Axial position-dependent fluxes calculated for the fuel region relative to the unperturbed flux in the fuel are shown in Figure 2.1, with bare foils inserted in the fuel rod. Similar calculated results, with cadmium covered foils inserted in the fuel, are shown in Figure 2.2. Additional calculations, with a bare 0.005-in. thick copper sector foil in the water, show a 0.6% thermal flux dip and a 0.2% epithermal flux dip in the foil when compared with unperturbed fluxes. These

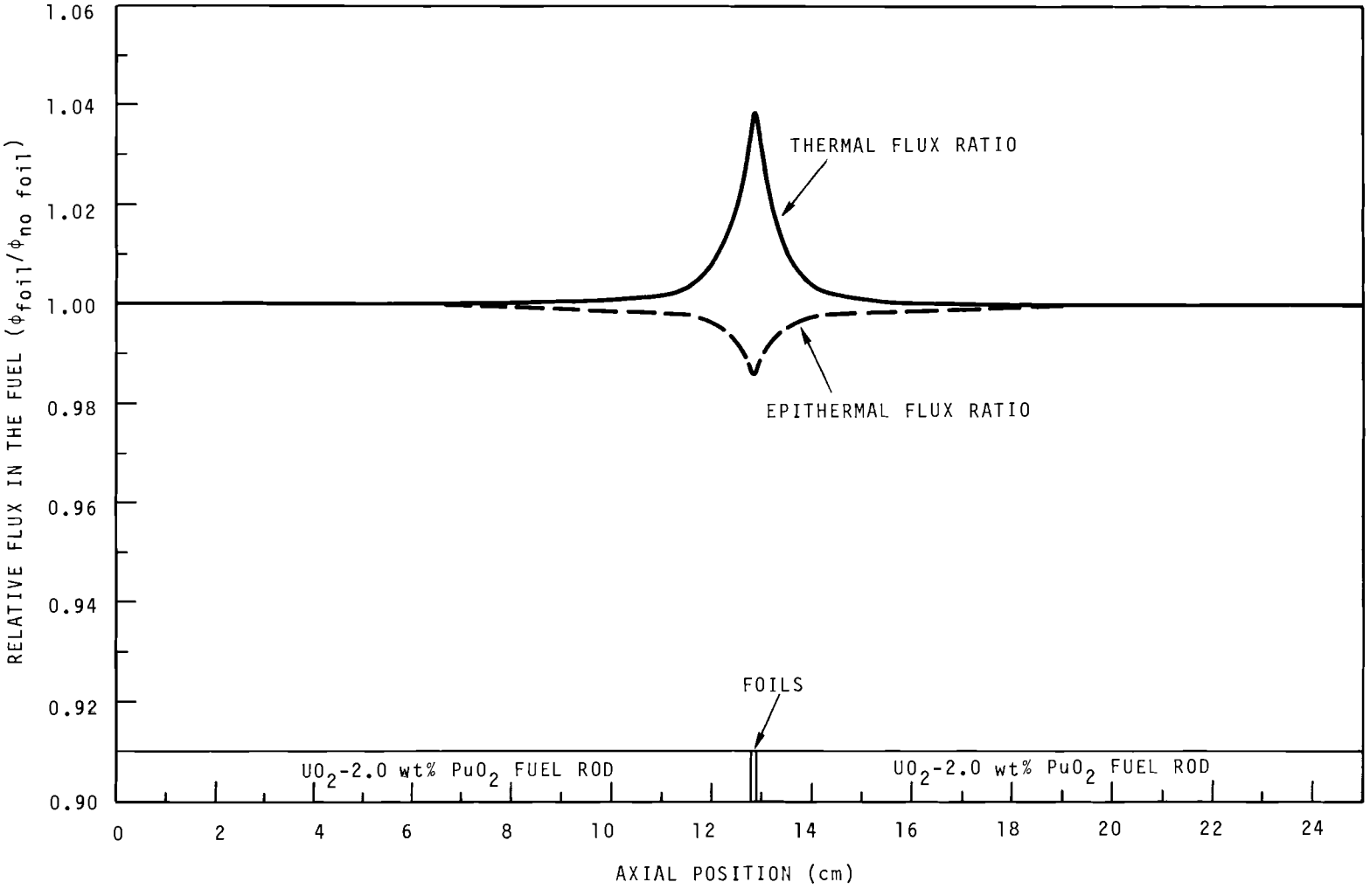

FIGURE 2.1. Neutron Flux Ratios for Bare Foils Irradiated in the Fuel

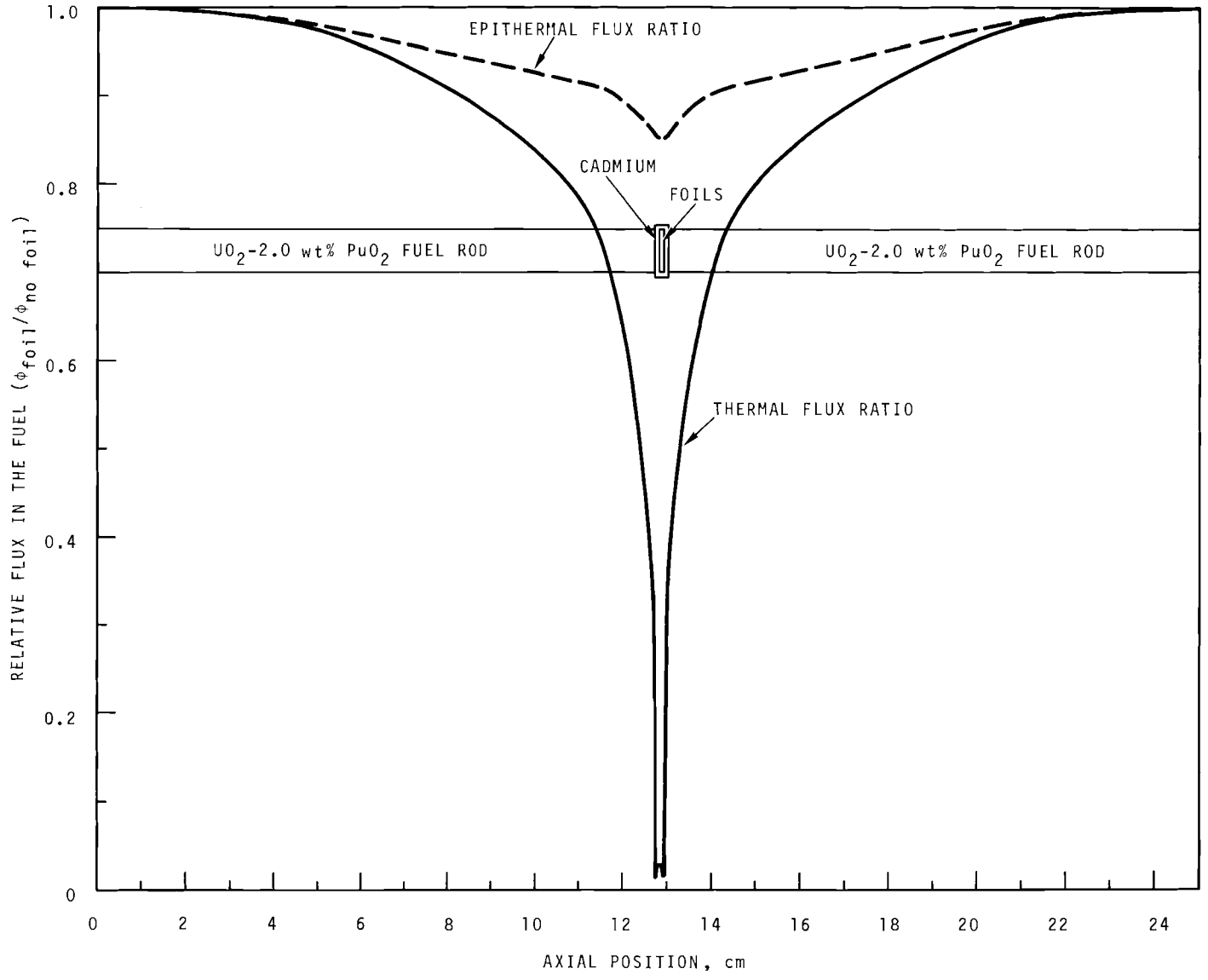

FIGURE 2.2. Neutron Flux Ratios for Cadmium Covered Foils Irradiated in the Fuel

foil perturbation correction factors were applied to the measured bare and cadmium covered foil activation rates to determine the reaction rates in the unperturbed central cell constituents.

PCTR Water Tank Calculational Model

As a means of (1) predicting neutron spectrum equilibration and central cell end effects, (2) identifying possible experimental problem areas, and (3) correlating experimental results, a PCTR calculational model can be a useful analytical tool. A two dimensional (R-Z) diffusion theory model of the PCTR, with the water tank installed in the central test region, was obtained by radial cylindrification of equivalent volumes for all PCTR zones. Using the 2 DB Code,[7] calculations were performed for the PCTR water tank experiment with UO_2-2.0 wt% PuO_2 rods.[2,3] The neutron spectrum in the vicinity of the central cell was matched to the fundamental mode value, as shown in Figure 2.3; the calculated radial spectral variation was in agreement with gold cadmium ratio measurements in the water tank. Comparison of the calculated axial variation of the thermal flux on the outer surface of the central cell fuel clad with measured subcadmium activation rates of 0.020-in. diameter gold pins on the clad surface, is shown in Figure 2.4. The good agreement in the thermal flux peaking in the ends of the lucite and polyethylene central cell containers builds confidence in the model. Thermal flux peaking in the ends of the central cell fuel rods was calculated to increase the axially averaged thermal flux in the fuel 1.9% over the value calculated at the reactor centerline. Replacing the plastic container ends with aluminum removed most of the moderating effect from the end cap planes, and reduced the axially averaged thermal flux in the fuel to a factor 1.006 times the value calculated at the reactor centerline.

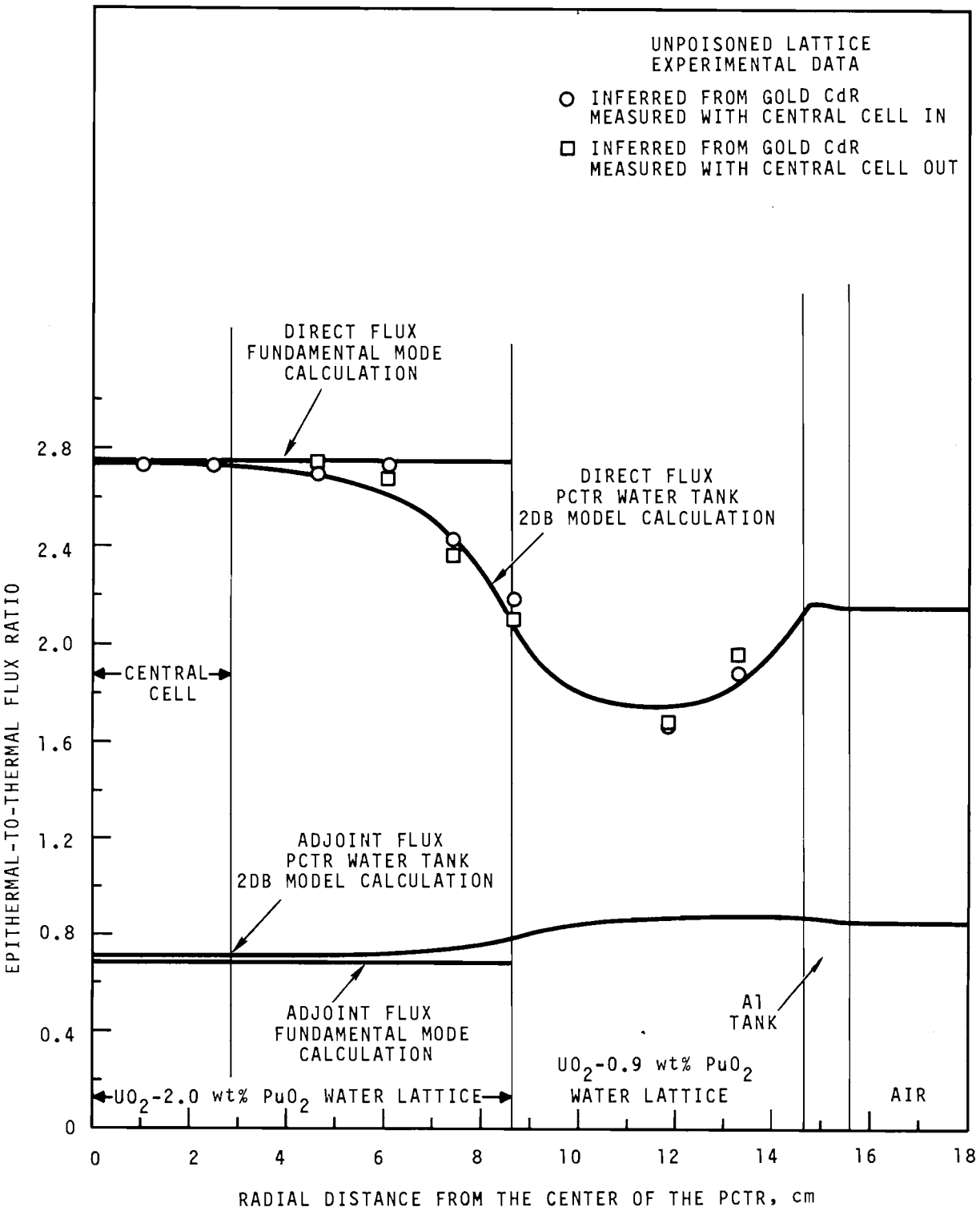

FIGURE 2.3. Neutron Spectrum Equilibration in the PCTR Water Tank

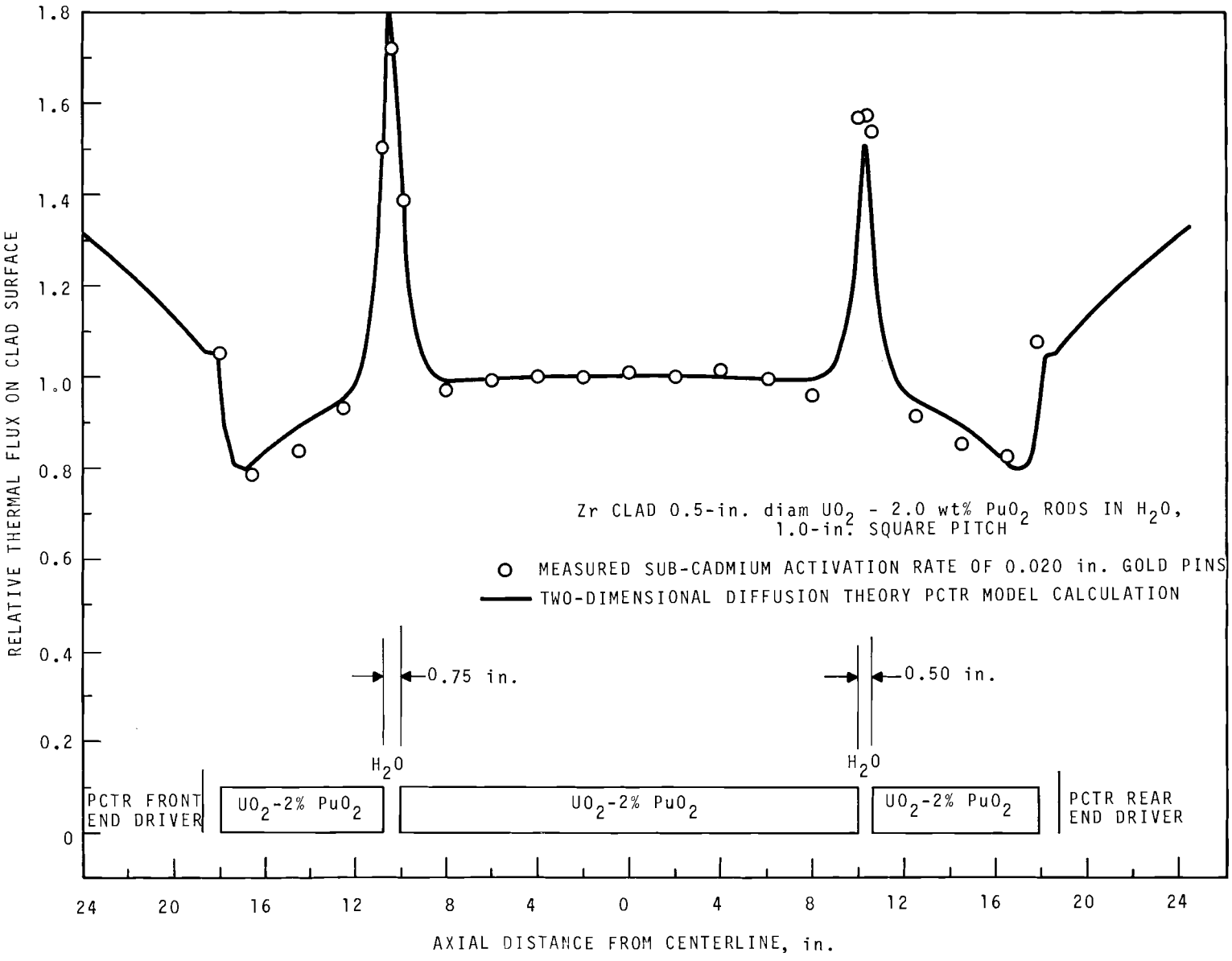

FIGURE 2.4. Axial Variation of Thermal Flux on the Outer Surface of the Fuel Clad

As a result of these studies, containers with aluminum ends have been fabricated for use with this water tank lattice. The null reactivity technique, using boric acid in the water at a concentration adjusted to give k_∞ of unity, will be used for the next set of experiments in this lattice in the PCTR.

Evaluation of k_∞

The value for k_∞ was determined from the experimental reactivity worth data and relative reaction rates in the unpoisoned lattice using the two group expression:[8]

$$k_\infty = 1 + \left(- \frac{\Delta\rho^{cell}}{\Delta\rho^{Cu}} \right) \frac{(\Sigma\phi V)_2^{Cu}}{(\Sigma\phi V)_2^{cell}} \left[1 + \frac{(\phi_1^+ \Sigma_1 \phi_1)^{Cu}}{(\phi_2^+ \Sigma_2 \phi_2)^{Cu}} \right]$$

$$- \frac{(1+\tau B^2)(1+L^2B^2)(1-p)L^2B^2}{1 + (1-p)L^2B^2} + \frac{\tau B^2 (1+L^2B^2) \left[\tau B^2 - \eta_1 f_1 (1-p) \right]}{1 + \tau B^2 - \eta_1 f_1 (1-p)}$$

The k_∞ defined in this expression is consistent with the two group fundamental mode calculation:

$$k_\infty = \frac{\text{Total Neutron Production}}{\text{Total Neutron Absorption}} = \frac{\nu_1 \Sigma_1^f \phi_1' + \nu_2 \Sigma_2^f \phi_2'}{\Sigma_1^a \phi_1' + \Sigma_2^a \phi_2'}$$

where ϕ_1' and ϕ_2' are equilibrium fluxes.

All measured and calculated quantities used in the evaluation of k_∞ are listed in Table 2.6. Using these values, the inferred value of k_∞ is:

$$k_\infty = 1 + (0.306 \pm 0.011) - (0.006 \pm 0.001) + (0.071 \pm 0.016)$$
$$= 1.371 \pm 0.019$$

TABLE 2.6. Quantities Used in the Evaluation of k_∞

Measured Quantities

$$\left(-\frac{\Delta\rho^{cell}}{\Delta\rho^{Cu}}\right) = \frac{85.819 \pm 0.057¢}{2.598 \pm 0.056¢} = 33.03 \pm 0.71$$

$$\frac{(\Sigma\phi V)_2^{Cu}}{\left(\phi_o\right)^{thermal}_{column}} = 13.72 \pm 0.13$$

$$\frac{(\Sigma_1\phi_1)^{Cu}}{(\Sigma_2\phi_2)^{Cu}} = 0.097 \pm 0.001$$

$$\frac{(\Sigma\phi V)_2^{cell}}{\left(\phi_o\right)^{thermal}_{column}} = 1585 \pm 40$$

Calculated Quantities

$\frac{\phi_1^+}{\phi_2^+}$	= 0.7115	2DB PCTR Model	
τ	= 30.74 cm^2	HRG	
p	= 0.8326	HRG	
$\eta_1 f_1$	= 0.6739	HRG	
L^2	= 2.090 cm^2	THERMOS	
$\eta_2 f_2$	= 1.507	THERMOS	
B^2	= 0.01157 cm^{-2}	HFN[9]	Fundamental Mode (Just Critical Bare Sphere)
$\frac{\phi_1'}{\phi_2'}$	= 2.748	HFN[9]	Fundamental Mode (Just Critical Bare Sphere)
$\frac{\phi_1}{\phi_2}$	= 2.734	2 DB PCTR Model	

Conclusion

The previously reported value for k_∞ - 1, determined by the unpoisoned technique, was 0.452 ± 0.015. The reevaluated k_∞ - 1 value of 0.371 ± 0.019 results from an accumulation of several small negative systematic errors which previously had been either neglected or improperly evaluated. Corrections for central cell end cap effects, thermal flux peaking in the ends of the plastic containers, activation foil perturbations, and the analytical model used to infer k_∞ resulted in reductions of 7%, 2%, 6%, and 2%, respectively, of the previously reported value for k_∞ - 1. The calculated values for k_∞ = 1.3646 from THERMOS-HRG-HFN[9] and k_∞ = 1.3645 from THERMOS-EGGNIT[10]-HFN are in excellent agreement with the value inferred from the experiment.

A considerable improvement in the precision of the k_∞ measurement is predicted if the null reactivity technique is used, since the relatively large epithermal leakage correction term in the unpoisoned k_∞ analytical model is eliminated. The uncertainty in k_∞ for the UO_2-2.0 wt% PuO_2 water lattice poisoned to null reactivity is estimated at ±0.003 in k_∞. An experiment to test this prediction of improved precision is planned for the near future.

References

1. *D. F. Newman, D. R. Oden, W. P. Walsh and A. D. Vaughn. "Water Moderated Test Lattices in the PCTR," Plutonium Utilization Program Technical Activities Quarterly Report, September, October, November, 1967, BNWL-654, pp. 3.10-3.23, Battelle-Northwest. February 1968.*

2. *D. F. Newman, D. R. Oden and A. D. Vaughn. "2 wt% PuO_2 Mixed Oxide Single Rod Experiments in the PCTR Water Tank," Reactor Physics Department Technical Activities Quarterly Report, April, May, June, 1968, BNWL-887, pp. 3.58-3.69, Battelle-Northwest. November 1968.*

3. D. F. Newman, D. R. Oden and A. D. Vaughn. "Measurement of Microscopic Neutronic Parameters in UO_2-PuO_2 Rods Moderated by Light Water," Plutonium Utilization Program Technical Activities Quarterly Report, September, October, November, 1968, BNWL-963, pp. 3.12-3.20, Battelle-Northwest. January 1969.

4. F. R. Mynot. Users Manual for DOT, K-1049, Available from Clearinghouse for Federal Scientific and Technical Information, Springfield, Virginia.

5. D. R. Skeen and L. J. Page. THERMOS/BATTELLE, The Battelle Version of the THERMOS Code, BNWL-516, Battelle-Northwest. September 1967.

6. J. L. Carter, Jr. "Effective Cross Sections for Resonances in HRG," and, "Computer Code Abstracts," Reactor Physics Quarterly Report, July, August, September, 1966, BNWL-340, Battelle-Northwest. October 1966.

7. W. W. Little, Jr. and R. W. Hardie. 2DB, a Two-Dimensional Diffusion Burnup Code for Fast Reactor Analysis, BNWL-640, Battelle-Northwest. 1968.

8. E. P. Lippincott, C. R. Richey and D. D. Lanning. "Definition of the Infinite Neutron Multiplication Factors Measured by the PCTR Poisoned and Unpoisoned Technique," Reactor Physics Quarterly Report, July, August, September, 1969, BNWL-1240, Battelle-Northwest. November 1969.

9. J. R. Lilley. Computer Code HFN - Multigroup, Multiregion Neutron Diffusion Theory in One Space Dimension, HW-71545, General Electric Company, Richland, Washington. November 1961. Available from Clearinghouse for Federal Scientific and Technical Information, Springfield, Virginia.

10. C. R. Richey. EGGNIT: A Multigroup Cross Section Code, BNWL-1203, Battelle-Northwest. November 1969.

BRT-I: BATTELLE-REVISED-THERMOS-I

C. L. Bennett and W. L. Purcell

1. Name: BRT-I (Battelle-Revised-THERMOS)

2. Computer: BRT-I is designed to operate on the UNIVAC 1108 computer system.

3. Problem Solved: The code computes the space dependent thermal neutron density, flux and current spectra over the energy range 0 to 0.683 eV in either slab or cylindrical geometry.

4. Method of Solution: The neutron density is computed from the collision probability form of the integral transport-theory matrix equation using either a combination of power iteration, overrelaxation and extrapolation or straight power iteration. The neutron currents are computed from either the gradient of the scaler flux or the uncollided flux matrix. The flux and current spectra is used to weight point thermal cross sections over an arbitrary thermal energy range for use in multigroup transport or diffusion theory codes.

5. Restrictions on the Complexity of the Problem: Number of space points ≤ 30, number of isotopes ≤ 30, number of speed points ≤ 30, number of material mixtures ≤ 8, slab or cylindrical geometry.

6. Typical Running Time: With the random access library: 1 min with a reflecting boundary condition and 30 sec with a white boundary condition. Succeeding cases using the same cross sections take about 15 sec each.

7. Unusual Features of the Code: White albedo boundary condition, current calculation, transverse buckling, linear anisotropic scattering correction, and smeared cell punched card output which can be used as region input for a

succeeding case, are several of the options available to the user. A random access library data element can be stored on drum or disk memory, if available, resulting in a considerable decrease in running time.

8. Related and Auxiliary Programs: RLITHE, updates and/or prints the BRT data tape or random access data element.

9. Status: BRT-I is in production use on the UNIVAC-1108 computer at Pacific Northwest Laboratory, Richland, Washington.

10. References:

- C. L. Bennett and W. L. Purcell, BRT-I: Battelle-Revised-THERMOS, BNWL-1434, Battelle-Northwest, 1970.
- H. C. Honeck. THERMOS, A Thermalization Transport Theory Code for Reactor Lattice Calculations, BNL-5826. Brookhaven National Laboratory, Upton, New York, September 1961.
- D. R. Skeen and L. J. Page. THERMOS/BATTELLE: The Battelle Version of the Thermos Code, BNWL-516, Battelle-Northwest. June 1967.
- J. E. Suich and H. C. Honeck. The HAMMER System, DP-1064, Savannah River Laboratory, Aiken, South Carolina, January 1967.
- B. J. Toppel and I. Baksys. The Argonne-Revised THERMOS Code, ANL-7023, Argonne National Laboratory, Lemont, Illinois, March 1965.

11. Machine Requirements: 64K memory, normal input, output, program, and punch units, 1 unit for library, 3 scratch units or their equivalent on drum.

12. Programming Language Used: FORTRAN-IV.

13. Operating System: UNIVAC-1108 computer with FORTRAN-V compiler and CSCX operating system.

14. User Information: The code and report may be obtained either through the Argonne Code Center at Argonne National Laboratory or from Pacific Northwest Laboratory in Richland, Washington.

15. Material Available: Magnetic Tape transmittal.
BRT-1 Source deck (approximately 3000 cards)
RLITHE Source deck (less than 1000 cards)
Library deck (8000 cards)
Sample problem (19 cards).

16. Acknowledgment: This work is based on work performed under U. S. Atomic Energy Commission Contract AT(45-1)-1830.

C. L. Bennett
W. L. Purcell
Reactor Physics Department
Battelle-Northwest
P. O. Box 999
Richland, Washington 99352

BMC-I: THE BATTELLE MONTE CARLO CODE

D. H. Thomsen

1. Name: BMC-I (Battelle Monte Carlo Code)

2. Computer: The BMC Code is designed to operate on the UNIVAC 1108 computer system. Approximately 65K words of core are required.

3. Problem Solved: The BMC code is a general purpose neutronic Monte Carlo Code. The code was developed primarily for use in solving some of the more complex problems encountered in predicting the neutronic characteristics of thermal reactors. Some of the problems which the BMC code has been used to solve are: lattice cell parameters such as resonance escape, thermal utilization, and cross section averaging, criticality problems, power distributions, shielding problems, and first flight collision probabilities.

   The BMC code is flexible as to the size and type of problem solved and in the cross section and geometry detail which may be used. The neutron fluxes and reaction rates in the energy range from 0 to 10 MeV are calculated in one, two, or three space dimensions. Statistical confidence limits are assigned to the results. The cross sections utilized in the BMC code are processed from data in the ENDF/B format.

4. Method of Solution: Analog Monte Carlo techniques are used to determine neutron histories. The neutron fluxes, reaction rates, and leakage are obtained from the histories by using an exponential track length estimator. Variance reduction techniques such as absorption weight ratioing, importance weighting, and Russian Roulette are also available.

The reactions which are treated are fission, capture, anisotropic, isotropic, and thermal elastic scattering, and inelastic n - n′ and n - 2n reactions. Thermal scattering makes use of the ideal gas model with a corrective technique to account for thermal binding effects.

The cross sections are defined using micro-group averaged cross sections. The resonance cross sections can also be treated at each energy using the Doppler broadened Breit-Wigner resonance formulae.

The geometry is defined using regions enclosed by planes, cylinders, spheres, or boundaries of the form $A(X - X_o)^2 + B(Y - Y_o)^2 + C(Z - Z_o)^2 - K = 0$. Provisions are made for voids and for reflecting symmetry boundaries. A general source routine is available for starting the neutrons. For eigen value problems the fission neutrons are used as the source. Statistics are obtained on all calculated quantities by processing batches and taking a standard deviation of the results from each batch. A special geometry routine is included for a square array of clad fuel rods. The fuel in each rod may be different.

The BMC code contains restart capability so that the results can be examined at a number of steps in the calculation.

5. Restrictions on the Complexity of the Problem: The BMC code was designed to make it easy to change the dimensions and hence make it available for a large range of problem types. A typical problem might have 5 materials, 30 geometry regions, 10 tally regions and 190 energy groups with 60 energy groups below 1.0 eV. However, problems have been run with 2 materials, 132 geometry and 132 tally regions and 96 energy groups and with 10 materials, 60 regions, 40 tally regions, and 190 energy groups.

One restriction is imposed by the approximate model used for the thermal scattering. It has been developed for light and heavy water at 293 °K. To use it at other temperatures or for other moderators requires a further special cross section preparation.

6. Typical Running Time: The running time for the BMC code as with all Monte Carlo Codes is very dependent on the complexity of the problem. The time varies from 2 to 10 min for the simplest problems up to several hours for the more complex problems. Typical times for single rod lattice cells would be in the range of 2 to 20 min while that for a power distribution in a fuel bundle would be in the range of 1/2 to 1 1/2 hr.

7. Unusual Features of the Program: The BMC code uses data in the ENDF/B format so use can be made of the ENDF/B data files. Also the BMC code does a complete energy calculation from fast to thermal.

8. Related and Auxiliary Programs: The BMC code is an update of the RBU Monte Carlo code which was coded in machine language for the IBM-7090-7094 computer system. The BMC code package consist of three codes: BMC, BMCLIB, and LIBR. BMC is the Monte Carlo code. The BMCLIB code is used to process cross sections from the ENDF/B format and prepare a cross section library for the BMC code. The LIBR code can be used to make corrections to or listings of the BMC cross section tape. The LIBR code makes use of the generalized input routine, NAMELIST.

9. Status: The BMC code is in production use of the UNIVAC-1108 computer at Pacific Northwest Laboratory, Richland, Washington.

10. References:

- D. H. Thomsen and T. M. Traver, BMC-I. The Battelle Monte Carlo Code, To be published, Battelle-Northwest.

- J. R. Triplett, E. T. Merrill and J. R. Burr. The BRU Reactor Burnup Code: Formulation and Operating Procedures, HW-70049, July 1961.

11. Machine Requirements: Approximately 65K words of directly addressable core storage are required by the program. Approximately 1,000,000 decimal words of scratch drum space are needed. Three tapes are needed in addition to the card reader and printer. A Calcomp plotter is required to exercise the plotting options of the code.

12. Programming Language Used: The program is coded primarily in Fortran-V (95%) and SLEUTH (5%).

13. Operating System: UNIVAC 1108 computer with Fortran-V compiler and CSCX operating system. The Calcomp plotter model 763 used for the plotting options.

14. Program Information: The BMC code and the BMCLIB code each consist of approximately 50 subroutines. They make use of overlay links to conserve on memory requirements. The LIBR code is a smaller code of approximately 12 subroutines. The entire code package is contained on about 14,000 cards.

15. User Information: The BMC code and report may be obtained either from the Argonne Code Center at Argonne National Laboratory or from Pacific Northwest Laboratory in Richland, Washington.

16. Acknowledgment: This work is based on work performed under U. S. Atomic Energy Commission Contract AT(45-1)-1830.

D. H. Thomsen
Reactor Physics Department
Battelle-Northwest
Box 999
Richland, Washington 99352

HRG-3

J. L. Carter

1. Name: HRG-3

2. Computer: The HRG-3 Code is designed to operate on the UNIVAC 1108 computer system.

3. Problem Solved: The code computes the slowing-down spectrum over the energy range 10 MeV to 0.414 eV in either the B-1 or P-1 approximation, using 68 groups of neutrons with a constant group width of delta u = 0.25. The calculated flux and current spectra are used to reduce the original 68-group cross section data to average values over as many as 32 broad groups.

4. Method of Solution: The 68 fine group fluxes and currents are calculated by one sweep through the group structure, starting from a specified source distribution. The source may be selected from among the 8 available on the data tape or may be read in. The multigroup model uses a full down-scattering matrix, with inelastic, n2n, and P0 and P1 components of elastic scattering explicitly included. Macroscopic fine group parameters are constructed from input nuclide concentrations and microscopic parameters, available on the data tape for more than 200 individual nuclides. There is no restriction, other than availability, on the number of nuclides usable in a case. A special calculation is made in the resonance range for certain nuclides, using an adaptation of the Adler, Hinman, and Nordheim method to an intermediate resonance approximation for both the absorber nuclide and an admixed moderator. The resonance contribution is allocated to the fine groups in a consistent manner providing self-shielding in both space and energy. Additional self-shielding factors may be read in for any nuclide, if desired. The fine group fluxes and currents

are used as weighting functions in averaging macroscopic and microscopic parameters over the specified broad group structure. Output is printed and may also be punched in formats for input to any of several spatial multigroup codes. As an option, the neutron age in an infinite medium may be calculated by the moments method.

5. Restrictions on the Complexity of the Problem: Number of broad groups ≤ 32. Broad group boundaries adjusted to coincide with one of the 68 fine group boundaries.

6. Typical Running Time: For 10 nuclides, including 4 with resonance calculation and no punched output, 40 sec for first case in a run, 20 sec for each succeeding case.

7. Unusual Features of the Program: The code strikes a balance between accuracy and speed at a level highly suitable for both survey and normal reactor design and analysis applications.

8. Related and Auxiliary Programs: NUTAPE-II, updates and/or prints the HRG data tape.

9. Status: HRG3 is in production use on the UNIVAC-1108 computer at Pacific Northwest Laboratory, Richland, Washington.

10. References:

- J. L. Carter, HRG3: A Code for Calculating the Slowing Down Spectrum in the P1 or B1 Approximations, BNWL-1432, Battelle-Northwest, 1970.
- G. D. Joanou and J. S. Dudek. GAM-I: A Consistent P_1 Multigroup Code for the Calculation of Fast Neutron Spectra and Multigroup Constants, GA-1850. General Atomics, San Diego, California, June 28, 1961.
- F. T. Adler, G. W. Hinman, and L. W. Nordheim. "The Quantitative Evaluation of Resonance Integrals,"

paper No. P/1988, Proceedings of the Second United Nations International Conference on the Peaceful Uses of Atomic Energy, vol. 16, pp. 155-171, United Nations, Geneva, 1958.

11. Machine Requirements: 64K memory, normal input, output, program, and punch units, 1 unit for library, 1 to 4 scratch units or their equivalent on drum.

12. Programming Language Used: FORTRAN-IV.

13. Operating System: UNIVAC-1108 computer with FORTRAN-IV compiler and CSCX operating system.

14. User Information: The code and report may be obtained either through the Argonne Code Center at Argonne National Laboratory or from Pacific Northwest Laboratory in Richland, Washington.

15. Material Available: Magnetic tape transmittal
HRG3 Source deck (approximately 3000 cards)
NUTAPE-II Source deck (approximately 1000 cards)
Sample problem (20 cards)
Library Data Tape.

16. Acknowledgment: This work is based on work performed under U. S. Atomic Energy Commission Contract AT(45-1)-1830.

J. L. Carter
Reactor Physics Department
Battelle-Northwest
P. O. Box 999
Richland, Washington 99352

DBUFIT-I: A LEAST SQUARES ANALYSIS CODE FOR NUCLEAR BURNUP DATA

R. P. Matsen

1. Name: DBUFIT-I

2. Computer: UNIVAC-1108

3. Problems Solved: DBUFIT-I is designed to extract integral cross section information from isotopic burnup data. This information is obtained by fitting burnup equations to the isotopic data using least squares fitting techniques. Burnup equations for the following transmutation chains have been encoded:

Transmutation Chain	Type of Fuel	Subroutine Name
$^{239}Pu \rightarrow {}^{240}Pu \rightarrow {}^{241}Pu \rightarrow {}^{242}Pu$	Pu	THEORY/PUAL
$^{238}U \rightarrow {}^{239}Pu \rightarrow {}^{240}Pu \rightarrow {}^{241}Pu \rightarrow {}^{242}Pu$	U + Pu	THEORY/URAN
$^{242}Pu \rightarrow {}^{243}Am \rightarrow {}^{244}Cm$	U + Pu	AMCM
$^{235}U - {}^{236}U - {}^{238}U = {}^{237}Np - {}^{236}Pu - {}^{238}Pu$	U + Pu	UCHAIN

4. Method of Solution: An iterative technique is used to find the best least squares fit of the transmutation equations to the measured burnup data. The values of the adjustable least squares parameters at this best least fit contain the desired integral cross section information.

5. Restrictions on the Complexity of the Problem: The data from as many as 150 samples may be analyzed at one time.

6. Typical Machine Time: Computational time depends upon the number of iterations required to obtain least squares convergence and the number of data points being fitted. On the UNIVAC-1108, a test case with nine data points requires approximately four seconds per iteration. Initial guesstimates for the fitting parameters are usually good enough that most problems converge in 25 to 50 iterations.

Doubling the number of data points doubles the running time per iteration. The only other significant use of machine time occurs during the generation of plotting information which may require up to thirty seconds for each plot. Timing information has been incorporated in the printed output so that the analyst can make good timing estimates for subsequent cases.

7. Unusual Features of the Program: The DBUFIT-I code provides for a simultaneous least squares fit of all transmutation equations in a given chain to the associated burnup data. One standard deviation uncertainties for all of the measured isotopes can be accommodated by the code.

8. Related and Auxilliary Programs: DBUFIT-I supercedes the DUBLIK code. Input is read in via the NAMELIST format. If need be, a comparable generalized input routine can be substituted for NAMELIST.

9. Status: DBUFIT-I is in production use at Pacific Northwest Laboratories on the UNIVAC-1108 computer at Richland, Washington.

10. References:
    - R. P. Matsen, "DBUFIT-I, A Least Squares Analysis Code for Nuclear Burnup Data", USAEC Report BNWL-1396, Pacific Northwest Laboratory, May 1970.
    - B. H. Duane, "Maximum Likelihood Nonlinear Correlated Fields (BNW Program LIKELY)", USAEC Report BNWL-390, Pacific Northwest Laboratory, September 1967.

11. Machine Requirements: Core memory requirements are 40,000 octal locations for instructions and almost 50,000 octal locations for data storage. The DBUFIT-I code consists of approximately 3500 card images and therefore is usually stored on either magnetic tape or drum. A card reader, printer and a card punch are also required. A CALCOMP plotter is necessary if plotted results are desired.

12. Programming Language Used: The program is written in UNIVAC FORTRAN-V.

13. Operating System: UNIVAC-1108 with FORTRAN-V compiler. The equipment and processing is under the control of Computer Sciences Conversational Executive (CSCX).

14. Other Programming Information: Computations are performed in double precision in order to avoid instabilities due to round off error by taking advantage of the efficient UNIVAC-1108 double precision hardware. With some decrease in efficiency and reliability, most cases can also be run in the single precision mode, thereby saving considerable data storage space in the core memory.

15. User Information: The DBUFIT-I code and report may be obtained from either the Argonne Code Center at Argonne National Laboratory or from Pacific Northwest Laboratory in Richland, Washington.

16. Acknowledgment: This code is based on work performed under U. S. Atomic Energy Commission Contract AT(45-1)-1830.

CODE DEVELOPMENT

G. D. Seybold

A computer code, GSSLRN-II, has been written which is an extension of the Code GSSLRN-I. Two primary differences are apparent. The first is that the user may now utilize the code for a general class of problems instead of being limited to one particular theory to describe his analytic peak shape. This generalization has already been proven by its application to Mössbauer spectra where the analytic peak shapes are described by a Breit-Wigner function. Secondly, the generalization has provided many new options which enable the user to manipulate input data and/or output results.

The code has been used routinely on both fission product spectra and Mössbauer spectra and has yielded results which have demonstrated that peak fitting of complex multiplets can be done on a routine basis with a high degree of success.

The code, GSSLRN-II, is still under development but is available for use in preliminary status if requested.

BURNUP CALCULATIONS FOR BNW 1 FUEL PINS

U. P. Jenquin

Introduction

Irradiation experiments on stainless steel clad mixed oxide (UO_2-PuO_2) fuels of various oxygen-to-metal ratios are being conducted in thermal reactors to study the system compatability and swelling of the fuel. Power and temperature distributions as a function of burnup are necessary to analyze the irradiation results. Physics calculations have been done to determine the power distribution in the BNW 1 fuel[1] at various exposures. Isotopic concentrations have also been determined as a function of burnup. The calculational results are normalized to operating data.

Description of Experiment

The fuel consists of UO_2-25 wt% PuO_2 clad in 304 SS. The uranium is of natural enrichment while the plutonium isotopic composition is 85.84/11.53/2.44/0.19 at.% Pu-239/240/241/242, respectively. The fuel rod is inserted into a capsule which is then inserted into one of the irradiation holes in the aluminum blocks in the MTR reflector. The capsule consists of annuli of NaK, 304 SS, and aluminum. A description of the fuel rod and capsule is summarized in Table 2.7.

TABLE 2.7. Description of Fuel Rod and Capsule

Composition	Outside Diameter, in.	Temperature, °C
Fuel	0.218	2300
304 SS	0.250	486
NaK	0.507	360
304 SS	0.568	232
NaK	0.692	179
Al	0.902	146
NaK	1.026	124
304 SS	1.124	87

Description of Calculation

The desired information from the physics analysis is: 1) isotopic concentrations of the fuel as a function of burnup, and 2) power distribution across the fuel at various exposures. Since the irradiations took place in the MTR reflector, nearly all of the power is due to thermal neutron induced fissions. Therefore, the burnup of the fuel can be approximately determined from power distributions and microscopic cross sections obtained from THERMOS/BATTELLE,[2] a multigroup transport code. The THERMOS code is designed to perform a space-energy calculation of thermal neutrons in a particular reactor cell geometry, but it will not perform isotopic transmutation calculations. Hence, the burnup code ZODIAC G[3] was incorporated into the

calculation. The ZODIAC G code has THERMOS as one of its modules, but this version of THERMOS does not allow sufficient geometric detail to obtain a sufficiently detailed power distribution for this work. Hence, the following calculational scheme was used to determine the physics parameters as a function of exposure:

1. A ZODIAC G burnup calculation was performed with a cell geometry of only one fuel region. This calculation provided isotopic fuel concentrations as a function exposure.
2. The ZODIAC G isotopic concentrations were then used as input to a THERMOS calculation which had a cell geometry containing five fuel regions. This calculation provided the power distribution across the fuel.

This scheme is discussed in more detail below.

THERMOS Cell Description

The space-energy distribution of thermal neutrons in the fuel was calculated with THERMOS. The "unit cell" used in the THERMOS calculation consists of eight regions. Region 8 (1.4 cm thick) contains equal volumes of aluminum and H_2O. The water adjacent to the aluminum block influences the neutron spectrum in the fuel. Region 7 contains the capsule and fuel clad which are homogenized into one region. The average NaK temperature was assumed to be 250 °C. The remaining six regions describe the fuel and a central void, as discussed below.

Shortly after irradiation is begun, the fuel forms a central void with the density of the fuel near this void increasing. From photomicrographs, the typical void diameter was estimated to be 60 mils. To determine the nuclear characteristics in detail, it is necessary to divide the fuel into a number of regions. Five fuel regions (2-6) were selected because of a limitation of eight mixtures in a THERMOS

calculation. The fuel region dimensions and densities are summarized in Table 2.8. Region 1 is the void.

TABLE 2.8. Description of Fuel Regions

Region	% of Fuel Radius	Outside Radius, cm	Thickness, cm	Fuel Density % of TD	Fuel Density g/cm^3
1 (VOID)	27.5	0.07620	0.07620		
2	50	0.13843	0.06223	98	10.868
3	70	0.19380	0.05537	98	10.868
4	85	0.23533	0.04153	95	10.536
5	93	0.25748	0.02215	92	10.203
6	100	0.27686	0.01938	92	10.203

ZODIAC G Calculation

Isotopic concentrations as a function of exposure were calculated with the burnup code ZODIAC G. In the ZODIAC G calculation, the fuel is not divided into regions, so the burnup is an average over the fuel. Ratios of cross sections do not vary significantly across the fuel, so the burnup path at any one position should be nearly the same as the average burnup path. Isotopic concentrations as a function of exposure were obtained for fuel of 92% TD and for fuel of 98% TD. The burnup steps are in increments of about 25,000 MWd/MTM. The isotopic concentrations were plotted as a function of expsoure for both fuel densities so that the isotopic concentrations at any desired expsoure could be determined quite readily. Isotopic concentrations for fuel at 95% TD were determined by interpolating between the curves for 98% and 92% TD fuel.

Power Distribution Calculation

To determine the power distribution and burnup across the fuel rod, a THERMOS calculation was done with the fuel divided into the five regions listed in Table 2.8. In order to perform this calculation it is necessary to determine the exposure of each fuel region at each burnup step. With this information,

the isotopic concentrations needed for each fuel region in THERMOS were obtained from the ZODIAC G curves described above. The incremental exposure of each fuel region was determined as the product of the relative power density of each fuel region times the incremental average exposure.

Power density is proportional to the product of macroscopic fission cross section and neutron flux. The relative power density in each fuel region is:

$$\bar{P}_r = \bar{\phi}_r \, \bar{\Sigma}^f_r \sum_{r=2}^{6} VF_r \Big/ \sum_{r=2}^{6} \bar{\phi}_r \, \bar{\Sigma}^f_r \, VF_r$$

where

$\bar{\phi}_r$ = region average thermal flux divided by the cell average thermal flux

$\bar{\Sigma}^f_r$ = region average macroscopic fission cross section

VF_r = volume fraction of region r relative to cell volume

$\sum_{r=2}^{6}$ = the summation over all fuel regions.

The denominator is just the cell average macroscopic fission cross section, $\bar{\Sigma}^f_{cell}$, calculated by THERMOS. In this nomenclature, the volume weighted averaged power density in the fuel is 1.0.

The power distribution was assumed to be constant through each burnup step. Hence, the average exposure that each region receives during each burnup step is just the region average relative power density, $\bar{P}_r$, times the incremental cell average exposure which was chosen as 25,000 MWd/MTM. The region average isotopic concentrations determined at the end of the one burnup step were then used in the five fuel region THERMOS calculation to determine the region average relative power densities to use in the next burnup step. The procedure was repeated until a cell average exposure of 150,000 MWd/MTM was reached. The accuracy of the results

would improve if a smaller incremental cell average exposure is used because the power distribution changes with burnup. All of the calculations included ^{135}Xe, ^{149}Sm, and a pseudo fission product.

Calculational Results

The power distribution for each burnup step is shown in Figure 2.5. The power distribution tends to become flatter with burnup because the concentration of fissile isotopes is depleted faster near the edge of the fuel where the thermal flux is much less than 1.0. Dividing the fuel into more regions would improve the results because the power density is not constant within a region as indicated in Figure 2.5.

The exposure distribution for each burnup step is shown in Figure 2.6. The exposure at the edge of the fuel is significantly higher than at the center of the fuel. If the burnup would be carried out to exposures well beyond 150,000 MWd/MTM, the curves would become flatter because the relative power density would become highest in the center of the fuel and the incremental exposure would be largest.

In order to calculate power distributions in THERMOS, the plutonium isotopic concentrations had to be determined for each region as a function of exposure. The total plutonium concentration for each region was calculated from the sum of the isotopic concentrations and plotted as a function of radius. The results are shown in Figure 2.7 for each burnup step. At low exposures the curves are not continuous because of the different fuel densities used in the regions. At high exposures this effect is washed out. These curves can be compared to measured plutonium distributions to assess the adequacy of the calculations. The average plutonium isotopic concentration at 75,000 MWd/MTM was calculated by volume weighting the isotopic

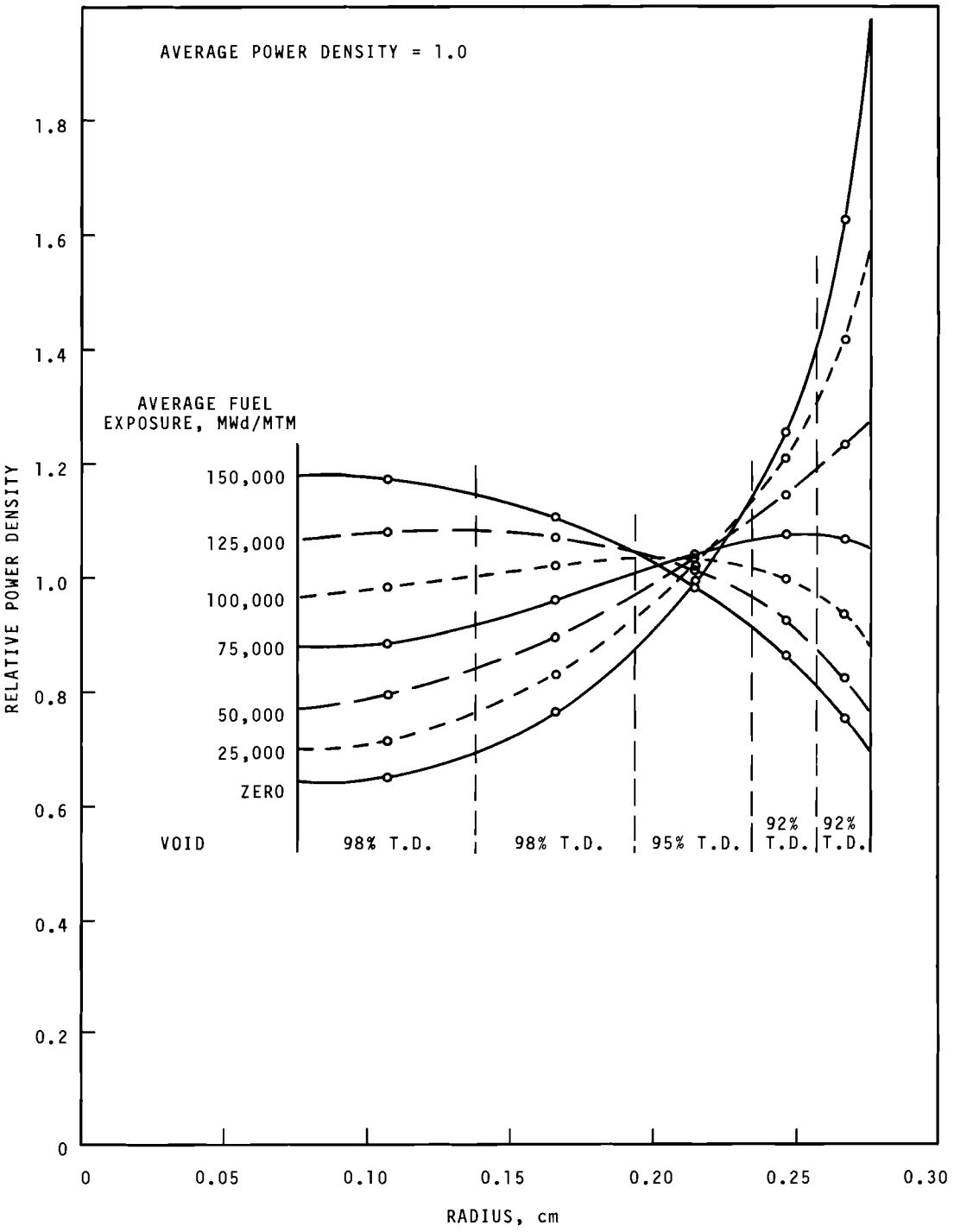

Neg 702765-1

FIGURE 2.5. Power Distribution in BNW 1 Fuel Pins

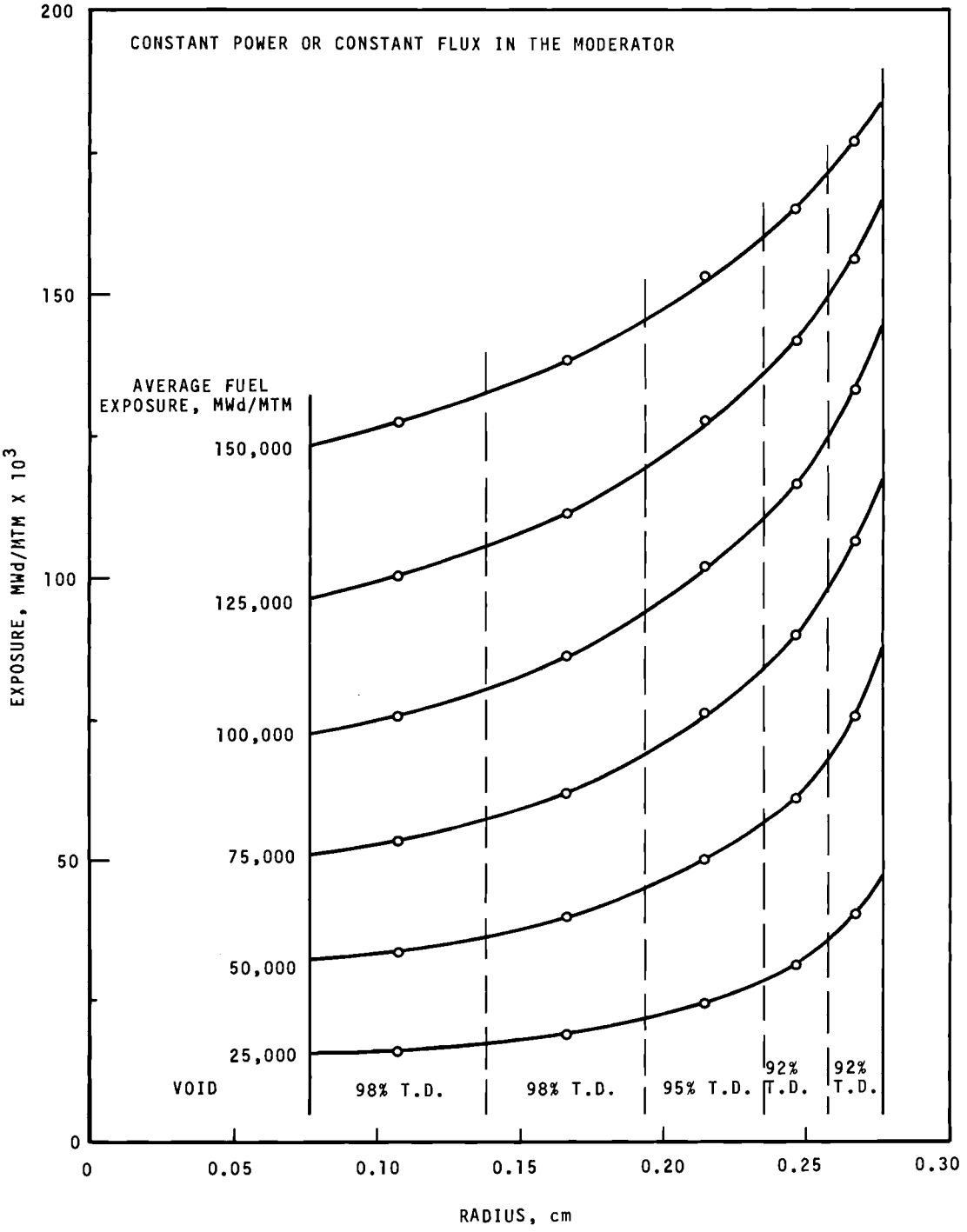

Neg 702765-2

FIGURE 2.6. Exposure Distribution in BNW 1 Fuel Pins

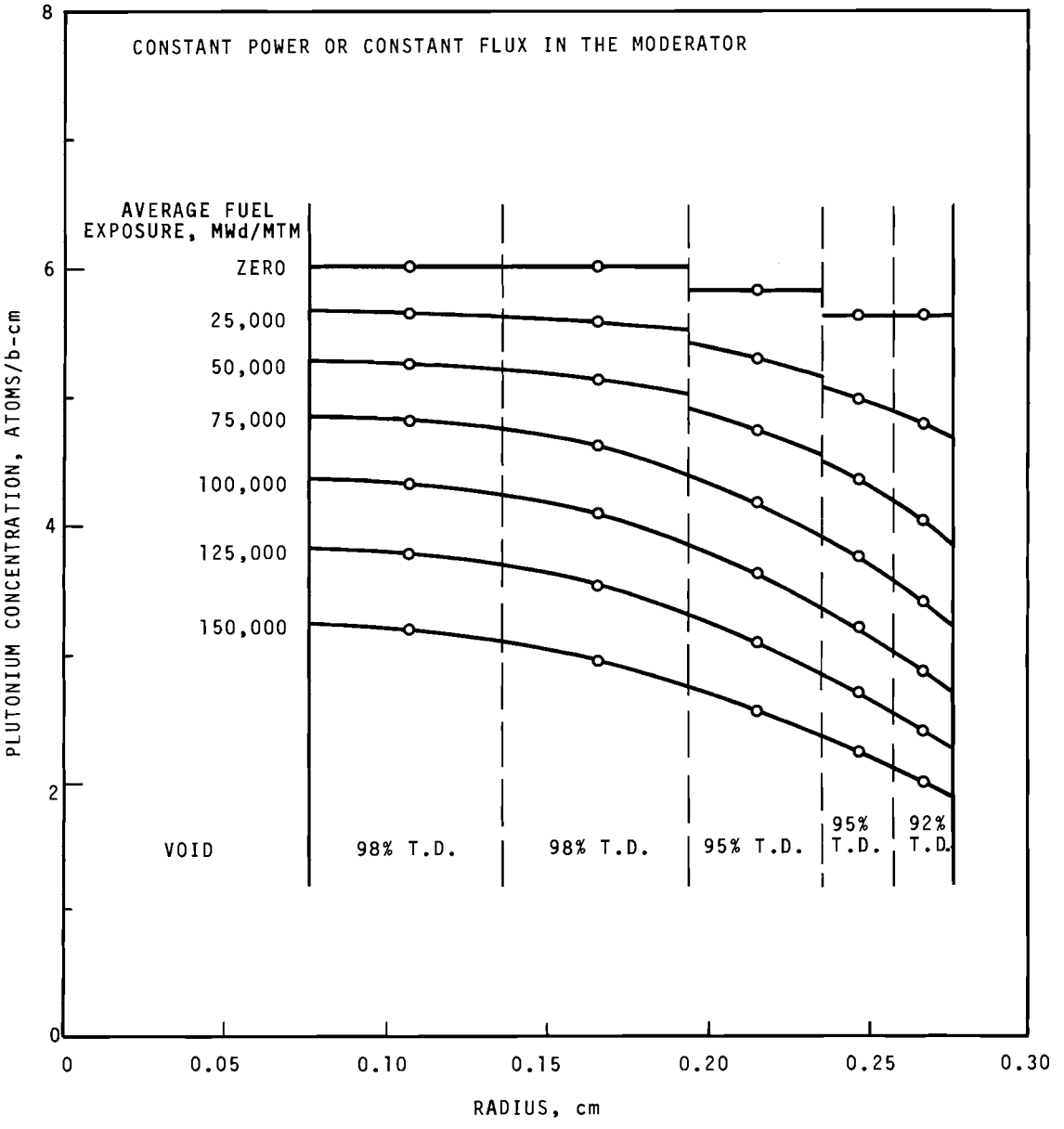

Neg 702765-1

FIGURE 2.7. Plutonium Distribution in BNW 1 Fuel Pins

concentrations for each region. The isotopic percentages are 66.6/26.1/6.1/1.2% Pu-239/240/241/242, respectively. A comparison with measured values will assess the accuracy of the ZODIAC G calculation.

Calculational Results Normalized to BNW 1-6 Fuel Pin

The irradiations took place in the MTR reflector where the thermal flux is contant with time. If the thermal flux outside of the fuel pin is constant, the power produced by the pin decreases with increasing exposure. The calculated results were normalized using measured data from BNW 1-6 which was irradiated to an average exposure of 75,000 MWd/MTM. Since exposure equals the product of power density and time, and the average exposure increments are all 25,000 MWd/MTM, the irradiation time for each burnup increment is inversely proportional to average power density. Thus, the irradiation time, ΔT, for each burnup increment is proportional to $\bar{\phi}_8/\bar{\Sigma}^f_{cell}$ where $\bar{\phi}_8$ is the average thermal flux in Region 8 and

$$\bar{\Sigma}^f_{cell} = \sum_{r=2}^{6} \bar{\phi}_r \, \bar{\Sigma}^f_r \, VF_r$$

is the cell average macroscopic fission cross section. Using the measured quantities of 75,000 MWd/MTM average exposure in 284.1 full power days for BNW 1-6, the time intervals were calculated by:

$$\Delta T(i) = 284.1 \, \bar{\phi}_8(i) \, \bar{\Sigma}^f_{cell}(i) \Big/ \sum_{i=1}^{3} \bar{\phi}_8(i) \, \bar{\Sigma}^f_{cell}(i)$$

where i refers to the burnup interval number. The quantity $\bar{\phi}_8(i) \, \bar{\Sigma}^f_{cell}(i)$ was assumed to be constant over the i^{th} burnup interval. The time intervals are calculated to be 89.6, 93.9, and 100.6 days for burnup Steps 1, 2, and 3, respectively. Knowing the time intervals to accumulate incremental average exposures of 25,000 MWd/MTM, the average power density was calculated by:

$\overline{P.D.}$ = average exposure times average fuel density/time interval

$\overline{P.D.}$ = 25,000 MWd/MTM 9.3301 g/cm^3/ΔT.

Once the average power density was determined, it was a simple matter to calculate the region average power density, by multiplying the average power density by the previously calculated relative power density for each region;

$\overline{P.D.}_r = \overline{P.D.}\ \overline{P}_r$.

The normalized, or absolute power distribution is plotted for the various burnup steps in Figure 2.8. The power density in the center of the fuel increases only slightly with exposure while at the edge of the fuel the power density decreases quite rapidly. The curves have the same shape as in Figure 2.5, but are renormalized to constant flux in the moderator rather than constant power in the fuel. Average power densities for the cell and the edge regions are plotted as a function of time in Figure 2.9. The change in power density with irradiation time or exposure is apparent. The cell average power density decreases gradually with time. On this graph the power densities are plotted at the midpoint of the time intervals because they are an average over the time interval.

Using the information to calculate absolute power densities, the absolute thermal flux in Region 8 was calculated to be 0.86×10^{14} n/cm^2-sec which is in excellent agreement with the measured MTR value of 0.9×10^{14} n/cm^2-sec.

Conclusions

The calculational model devised for the burnup of BNW 1 capsules seems to give reasonably good results. Very few checks have been made to assess the accuracy of the model. No detailed comparisons were made with experimental data. To eliminate most of the assumptions in the analysis would require a very sophisticated calculational model. A few simple

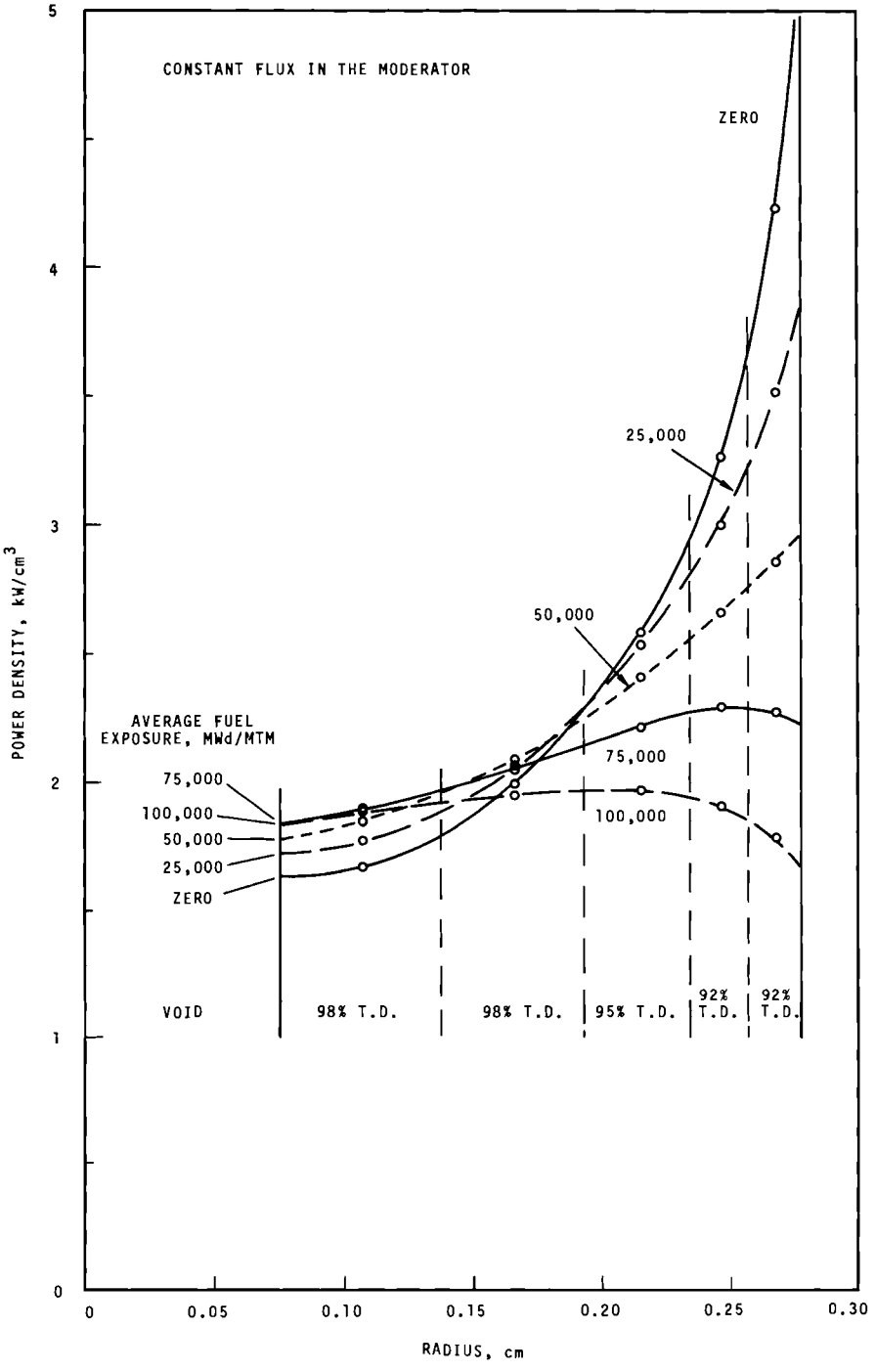

Neg 702765-4

FIGURE 2.8. Absolute Power Distribution in Fuel Pin BNW 1-6

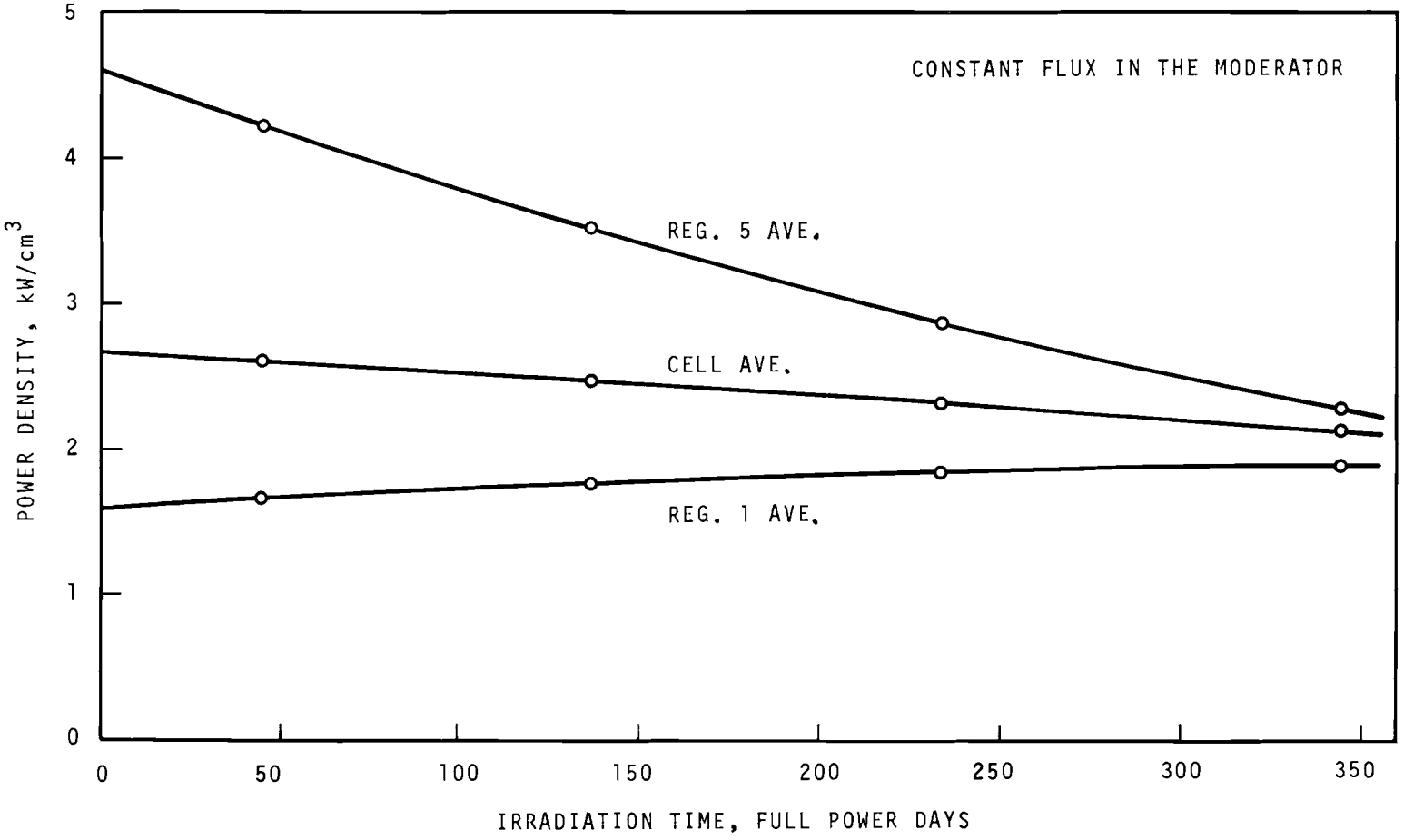

Neg 702756-5

FIGURE 2.9. Absolute Power Densities Versus Irradiation Time for Fuel Pin BNW 1-6

calculations were done to check some of the assumptions. The ratio of microscopic cross sections as a function of radius, fuel density, and exposure was investigated. The relative power density and exposure was calculated for various positions and compared to values at those positions obtained by drawing curves through the region average values. The adequacy of the space-energy flux distribution calculated with THERMOS was also investigated. These investigations indicated that no serious errors were made in the associated assumptions.

Areas which have not been investigated that could affect the results are:

- Assumptions associated with the ratio of nonthermal-to-thermal flux,
- Size of the burnup increments,
- Number of regions the fuel is divided into,
- Nonhomogeneity effects of the fuel.

References

1. *L. A. Pember. Unpublished Data. Battelle-Northwest, Richland, Washington, September 1967. (Proposal to Irradiate Mixed Oxide Stoichiometry Test Capsules.)*

2. *D. R. Skeen and L. J. Page. THERMOS/BATTELLE: The Battelle Version of the THERMOS Code, BNWL-516, Battelle-Northwest. September 1967.*

3. *D. D. Matsumoto and R. H. Holeman. "ZODIAC G," Reactor Physics Department Technical Activities Quarterly Report, January, February, March 1968, BNWL-775, Battelle-Northwest. July 1968.*

k_∞ MEASUREMENT FOR A ThO_2-$^{235}UC_2$-C HTGR LATTICE AS A FUNCTION OF TEMPERATURE

T. J. Oakes and C. R. Richey

Values for the infinite neutron multiplication factor as a function of temperature, $k_\infty(T)$, for a ThO_2-$^{235}UC_2$-C HTGR lattice have been obtained both by HTLTR measurement and by calculation. This lattice has been previously described in an earlier quarterly report.[1]

The observed reactivity worths of the HTGR cell and a standard absorber (Cu), as measured in the HTLTR, together with foil activation data, have been used to deduce k_∞ via the unpoisoned technique.[2] The expression used for this evaluation is:

$$k'_\infty = 1 - \left(\frac{\Delta\rho_{cell}}{\Delta\rho_{Cu}}\right) \frac{(\Sigma_{a_2} V\phi_2)_{Cu}}{(\Sigma_{a_2} V\phi_2)_{cell}} \left\{1 + \left[\frac{\phi_1^+}{\phi_2^+}\right] \frac{(\Sigma_{a_1}\phi_1)_{Cu}}{(\Sigma_{a_2}\phi_2)_{Cu}}\right\}\left[k^*\right]$$

$$- \frac{(1 + B^2)(1 + L^2B^2)(1 - p)L^2B^2}{1 + (1 - p)L^2B^2} \qquad \left[f_1(L^2B^2)\right]$$

$$+ \frac{\tau B^2(1 + L^2B^2)\ \tau B^2 - \eta_1 f_1(1 - p)}{1 + \tau B^2 - \eta_1 f_1(1 - p)} \qquad \left[f_2(\tau B^2)\right]$$

$$+ \frac{\Delta\Phi}{\Phi} \cdot \frac{\Delta\phi^+}{\phi^+} \cdot \tau B^2 \left(\frac{\Delta\phi^+}{\phi^+} - \frac{\Delta\phi}{\phi}\right) \qquad \left[g(\phi,\phi^+)\right]$$

where the first term, k*, is the result normally derived from an HTLTR-PCTR type experiment, $f_1(L^2B^2)$ and $f_2(\tau B^2)$ are terms which correct for the finite leakage present in the unpoisoned lattice, and $g(\phi,\phi^+)$ is a correction which arises because the direct flux and the adjoint flux spectra in the test array are not necessarily identical with the spectra present in a just

critical HTGR medium. If there is no mismatch between the fluxes in the void and the equilibrium fluxes characteristic of the medium, the terms

$$\Delta\phi = \left(\frac{\phi_1}{\phi_2}\right)_{void} - \left(\frac{\phi_1}{\phi_2}\right)_{medium} \quad \text{and} \quad \Delta\phi^+ = \left(\frac{\phi_1^+}{\phi_2^+}\right)_{void} - \left(\frac{\phi_1^+}{\phi_2^+}\right)_{medium}$$

go to zero. Similarly, as the buckling, B^2, of the unpoisoned lattices approaches zero ($k \to 1$), the $f_1(L^2B^2)$ and $f_2(\tau B^2)$ correction terms approach zero.

A summary of the values of $k_\infty'(T)$ as derived from the experiments in HTLTR is presented in Table 2.9. It must be remembered that of the measured quantities in the expression for k_∞^*, only the $\Delta\rho^{cell}/\Delta\rho^{Cu}$ ratio could be measured at elevated temperatures. The absorption rates in cell components, flux mismatches and leakage corrections at elevated temperatures were obtained from calculations which had been normalized to obtain agreement with the experimental data at room temperature.

The results listed in Table 2.9, also include the infinite neutron multiplication factors for the HTGR array as calculated by two group theory, i.e.,

$$k_\infty' = \frac{\nu\Sigma_1^f\phi_1' + \nu\Sigma_2^f\phi_2'}{\Sigma_1^a\phi_1' + \Sigma_2^a\phi_2'}.$$

TABLE 2.9. $k_\infty'(T)$ for a ThO_2-$^{235}UC_2$-C Lattice

T, °C	k_∞', Measured	k_∞', Calculated
20	1.111	1.0929
150	1.0925	1.0780
300	1.0760	1.0646
550	1.0487	1.0484
700	1.0377	1.0417
1000	1.0245	1.0285

The Σ_i^a and Σ_i^f in the above expression are the i^{th} group cell-averaged absorption and fission macroscopic cross sections, respectively, with ϕ_1' and ϕ_2' being the fast and thermal fluxes, respectively, from a fundamental mode calculation. A two group diffusion theory[3] calculation was utilized for the fundamental mode problem. The fast group constants, Σ_1^a and Σ_1^f, were computed by the EGGNIT slowing down code[4] using the B_1 calculation. Resonance self shielding was treated by the Northeim integration scheme in granular HTGR geometry.[5,6] Thermal group constants, Σ_2^a and Σ_2^f were obtained from a modified version[7,8] of the THERMOS[9] code for treating the HTGR granular fuel elements.

The measured change in k_∞ between 20 °C and 1000 °C is slightly larger than the corresponding calculated change but the agreement is generally good.

References

1. *T. J. Oakes. Reactor Physics Quarterly Report, January February, March 1970, BNWL-1381-1, p. 3.16, Battelle-Northwest. May 1970.*

2. *E. P. Lippincott, C. R. Richey, and D. D. Lanning. Reactor Physics Quarterly Report, July, August, September 1969, BNWL-1240, p. 2.3, Battelle-Northwest. November 1969.*

3. *J. R. Lilley. Computer Code HFN - Multigroup, Multiregion Neutron Diffusion Theory in One Space Dimension, HW-71545, General Electric Company, Richland, Washington, November 1961. Available from the Clearinghouse for Federal Scientific and Technical Information, Springfield, Virginia.*

4. *C. R. Richey. EGGNIT: A Multigroup Cross Section Code, BNWL-1203, Battelle-Northwest. November 1969.*

5. *L. W. Nordheim. The Theory of Resonance Absorption, GA-638 (Revised), General Atomic Division, San Diego, California. 1959.*

6. *R. K. Lane, L. W. Nordheim, and J. B. Sampson. Nuclear Science and Engineering, vol. 14, pp. 390 to 396. 1962.*

7. *C. L. Bennett. "Multiple Region Interaction Probabilities for Particle Size Theory," Reactor Physics Quarterly Report, July, August, September, 1968, BNWL-921. December 1968.*

8. *C. L. Bennett. "A Dipping and Peaking Correction for Particle Size Foils Used in Particle Fission Rate Density Measurements in Granular Fueled Lattices," Reactor Physics Quarterly Report, October, November, December, 1968, BNWL-985. Battelle-Northwest. February 1969.*

9. *H. C. Honeck. THERMOS, A Thermalization Transport Code for Reactor Lattice Calculations, BNL-5826, Brookhaven National Laboratory, Upton, New York. 1961.*

HTLTR TEMPERATURE COEFFICIENT

E. P. Lippincott

In planning for the second HTGR experiment in the HTLTR (High Temperature Lattice Test Reactor) it was necessary to estimate the temperature coefficient of the reactor in order to adjust the excess reactivity to enable the reactor to be taken critical at all temperatures. Methods of adjusting the temperature coefficient include varying the positions of the reactor loading and the addition of Gd_2O_3 poison shim rods which have a positive coefficent.

In the initial experiments in HTLTR it was observed that at temperatures slightly above room temperature, the reactor had a positive temperature coefficient. As the temperature was increased, the coefficient passed through zero and became increasingly negative. This latter effect was only partially compensated by Gd_2O_3 shims. Accordingly it was necessary to add reactivity to operate at the higher temperatures and the fuel-poison columns (FPC) were constructed for this purpose.(1)

To estimate the temperature coefficient and reactivity loss to 1000 °C, the 2-DB code was used, with a 2-group, 2-dimension calculational model of the HTLTR which had been adjusted to give the correct temperature coefficient for the first HTGR

lattice.[2] Calculations with this model were also performed to estimate the adequacy of the flux match across the HTGR test lattice. Several sets of calculations were performed with different fuel and gadolinium shim loadings. The calculations for loadings similar to the previous lattice gave a similar reactivity drop from room temperature to 1000 °C (about 2.60$). However, the calculations did not reproduce the initial reactivity increase.

Further calculations were done with the gadolinium shims moved radially outward and driver fuel moved inward. These adjustments improved the predicted flux match and resulted in a calculated reactivity loss of 4.85$. Eight additional gadolinium shims were added to the model but this resulted in a calculated decrease of 4.45$ at 1000 °C. Since the calculation was suspect, this last loading was tried in the HTLTR. It was found experimentally that the reactivity increased rapidly with the increasing temperature and it became necessary to remove some driver fuel from the reactor in order to operate.

The variation of the excess reactivity of the HTLTR as a function of temperature after this fuel removal is shown in Figure 2.10. The point at 25° is an estimate based on the amount of fuel removed. At temperatures of 750 °C and above, reactivity was added via the fuel poison columns to obtain an excess reactivity adequate to permit measurements.

Inspection of Figure 2.10 shows that a good loading has been established for operation over the full range from room temperature to 1000 °C. The total loss in reactivity from 20 to 1000 °C is only about 40¢. The maximum change in reactivity is from 400 to 1000 °C and has been held to 1.45$.

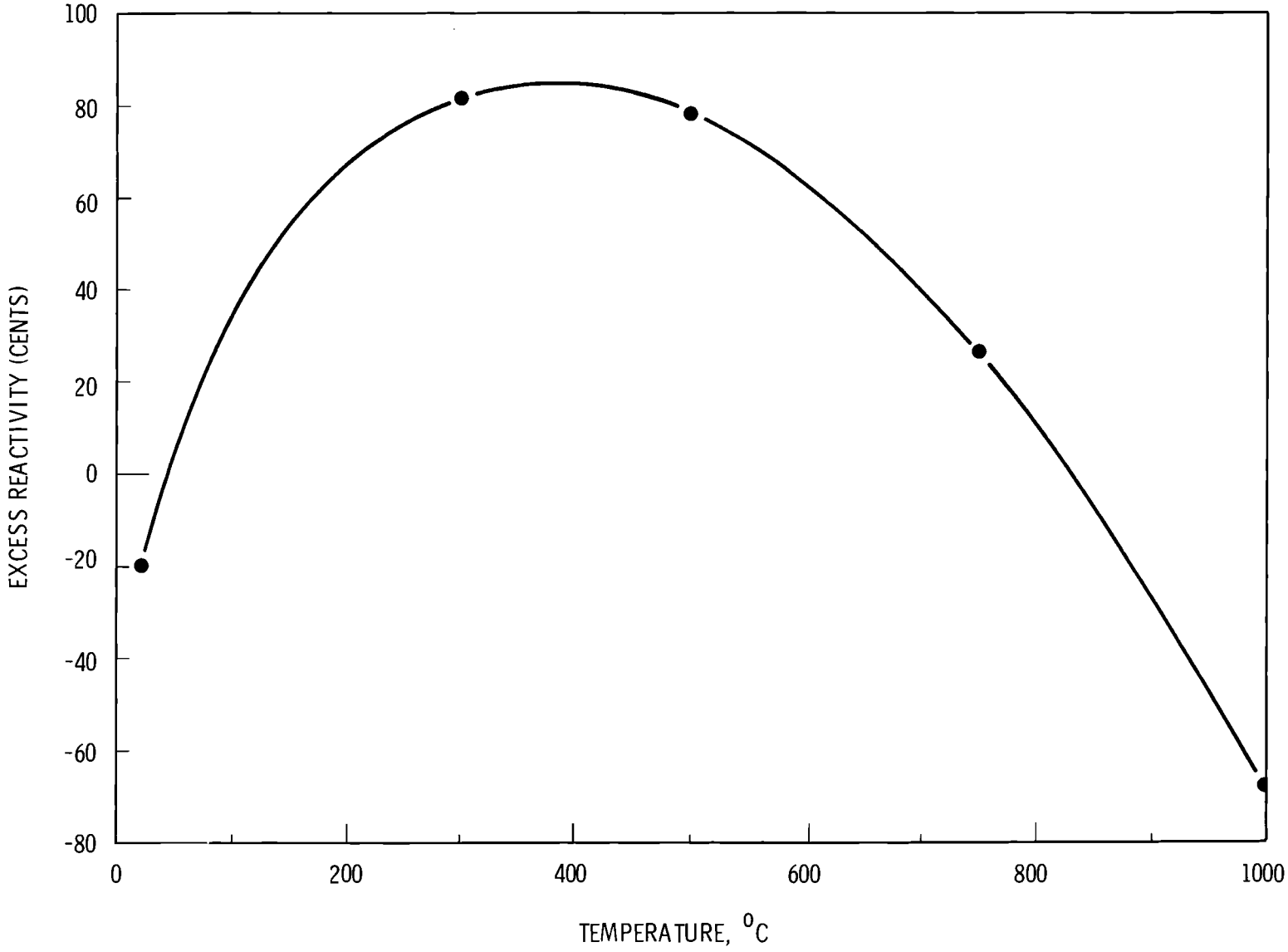

FIGURE 2.10. HTLTR Excess Reactivity

The temperature coefficient may be determined at each operating temperature from the slope of the curve in Figure 2.10. Since these coefficients were necessary for data correction, they were also determined at each temperature level by changing the reactor temperature by about 10 °C and measuring the reactivity change. The measurements by the two methods are compared in Table 2.10. Good agreement is obtained at 500 and 750 °C where the slope measurements are most accurate. Reasonable agreement is obtained at the other temperatures.

TABLE 2.10. HTLTR Temperature Coefficient

Temperature, °C	Measured Temperature Coefficient, ¢/°C	Temperature Coefficient from Slope in Figure 2.10, ¢/°C
20	+0.81	+0.88
150	+0.29	+0.32
300	+0.103	+0.082
500	-0.118	-0.120
750	-0.28	-0.29
1000	-0.51	-0.43

In future HTLTR experiments, it will be desirable to use loadings with temperature behaviors similar to the last experiment. It has been shown that the temperature coefficient can be adjusted by adding more gadolinium and moving it outward in the reactor. The HTLTR calculational model, while satisfactory for predicting flux matches in the test core, is unsatisfactory for estimating overall reactor temperature coefficients. Thus, future loadings will have to be designed based on empirical estimations until a more sophisticated model is developed.

References

1. *J. G. Holt. "Manual Reactivity Adjustments in HTLTR at Temperatures up to 1000 °C," Reactor Physics Quarterly Report, October, November, December, 1969, p. 3.15, BNWL-1304, Battelle-Northwest. February 1970.*

2. *C. R. Richey. Unpublished Data. Battelle-Northwest. (Personal Communication)*

HTLTR REACTOR PRESSURE CONTROL

W. C. Roberts

A fused quartz precision gage with a resolution to the nearest 0.005 Torr, has been interfaced with the program measurement and control system (PMACS) at the High Temperature Lattice Test Reactor (HTLTR). This instrument is used for high precision read out by the computer and a closed loop pressure control for the reactor.*

A computer program has been written and tested which has the capability of maintaining pressure automatically to within less than ±0.01 Torr. This finite pressure control was made possible through the versatility of computer control where each controller (program) can be designed for the characteristic of a given system. The method of pressure control was largely derived from previous operating experiences while controlling by manual manipulation of the control valves. Manual operation was necessary previously since a conventional control program was unable to provide the needed pressure stability necessary for nuclear experimentation. During these periods of operation the two most important variables were the responsiveness of the valve to a given minute change and deadband caused by the mechanical control linkage on a given valve.

The position range of the control valves are 0 to 100% open in units of 0.1% as determined by an electropneumatic valve positioner which receives a digital signal from PMACS. It was determined through previous operating experience that

* *Gas volume for the reactor system is 1000 scf.*

the valve could not be adjusted in 0.1% steps. Although the digital positioner would regulate the pneumatic control air to the valve, it would not respond until combined steps of up to 0.5 to 1% were received. Consequently, pressure control would over react to the calculated change. This problem was overcome by first moving the valve in the reverse direction to a position in which the valve would actually move about 0.5% (this is determined by the deadband plus 0.5%) and then after a set time delay it is repositioned to the calculated position called for by the control program. Following this sequence it then becomes possible to position the valve in 0.1% steps and pressure control becomes more responsive to minute changes. The control program will always add the valve deadband to the control position whenever the valve is set in the direction opposite from its last movement. This method of control eliminates the inherent problem of mechancial deadband within a given valve.

It was determined that the system pressure response to a given valve change was between 4 and 5 sec to see a change and 9 to 10 sec to come to equilibrium. For this reason, the program sampling interval was set to 9 sec. A shorter sampling interval caused the control program to over-correct and a longer interval allowed the pressure to drift from the set point.

Two valves are currently programmed to control reactor system pressure. The operator can set the system purge to a fixed amount by setting flow valve (2FCV12) to a set position, and pressure will be controlled using the makeup valve (2PCV12) or the makeup valve can be set and the program will control pressure by adjusting the purge valve.

The interfacing of the precision pressure gage with the PDP-7 process computer, and the development of the special software programs permit control of the reactor atmosphere

pressure to within ±0.01 Torr of a preselected set point automatically. This precise control of the nitrogen pressure reduces or eliminates the need for corrections to reactivity data due to variations in pressure between or during measurements.

CALCULATIONS OF HTLTR SAFETY ROD TEMPERATURE DISTRIBUTIONS

E. P. Lippincott

Introduction

The second series of reactivity measurements to 1000 °C in the HTLTR was recently completed. In this run, a modified design of the Vertical Safety Rod (VSR) was used in an attempt to correct heat expansion problems experienced in the first series. These rods are composed of 1/16-in. thick plates of nickel impregnated with Gd_2O_3 and Eu_2O_3 which are held in place by a frame of TD nickel rods (see Figure 2.11). These plates were found to have buckled due to expansion, thereby causing reduced clearance in the slot in which they were inserted. The buckling of the plates is apparently caused by stress due to internal temperature gradients in the plate since sufficient clearance in the slots was allowed for expansion. In order to calculate the gradients in the plate, a computer program, TEMP, was written. This program can be used to calculate the temperature distribution in the present VSR and to calculate the effect of proposed modifications.

Description of Calculation

The heat flow equation

$$-k \nabla^2 T + C\rho \frac{\partial T}{\partial t} = \sigma\varepsilon(T_o^4 - T^4)$$

is solved using TEMP. The T is the absolute temperature, k is the heat conductivity of the material, C is the specific heat, ρ is the density, σ is the Stefan-Boltzman constant for radiant heat transfer, T_o is the hot reactor temperature, and ε is the

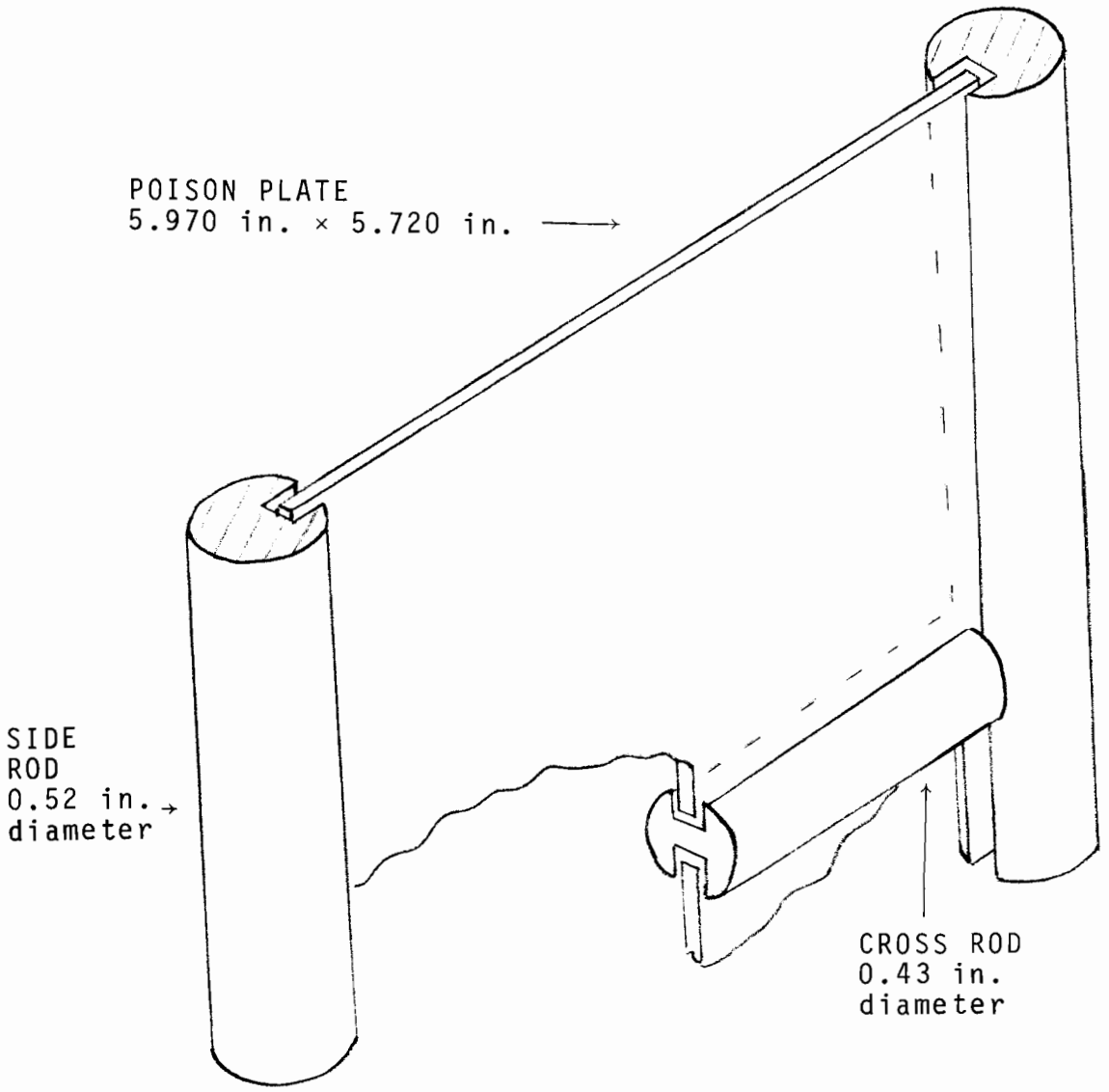

FIGURE 2.11. Arrangement, Plates and Frame, HTLTR VSR

effective emissivity. In this equation, the $k \nabla^2 T$ term represents the heat transferred by conduction and the $\sigma\varepsilon (T_o^4 - T^4)$ term is the heat transferred in by radiation. To solve this equation, the plate and rods are compressed to two dimensions and divided into a rectangular array of mesh points, and a difference technique is used. Each mesh point is identified as belonging to a region (in the simple case there are three regions--plate, side rod, and cross rod), and each region is supplied with parameters: density, thickness, heat conductivity to mesh points in the same region and to points in continuous regions, and emissivity. It was assumed that each material had the same specific heat, which was taken from a table in 100 °C increments.

With the above assumptions, the equation for the temperature at a point on the plate at time $t + \Delta T$ is given in terms of the temperature at time t by the relation:

$$T(t + \Delta t) = T(t) + \frac{\Delta t}{C \cdot D} A(T_o^4 - T^4) + \sum_{i=1}^{4} K_i (T_i - T).$$

The D is the density times the thickness, C is the specific heat of the material, A is 2 σ times ε and K_i is the thickness times the heat conduction coefficient to each of the four neighboring points included in the sum. The general parameters used are given in Table 2.11.

Results for Reference Case

The calculation of the present design of VSR at 20 °C inserted into a 1000 °C cavity is called the reference case. For this calculation, the plate was assumed to be in good contact with the cross rods and side rods (i.e. the heat conduction from the plates to the rod was assumed equal to the conduction from point to point in the plate.) Since the rods heat up more slowly than the plate, the rods act as a heat sink, cooling the edges of the plate. This case should be regarded

as exaggerating the temperature gradient since in the real case the contact between the plates and rods is less than perfect. In addition, the initial temperature was assumed to be 20 °C which is very conservative. The parameters used for the reference case are shown in Table 2.12.

TABLE 2.11. General Parameters Used in Temperature Calculations

Temperature, °C	Specific Heat of Nickel (C) cal/g °C
0 to 100	0.105
100 to 200	0.114
200 to 300	0.125
300 to 400	0.142
400 to 500	0.125
500 to 600	0.126
600 to 700	0.133
700 to 800	0.141
800 to 900	0.147
900 to 1000	0.152
Emissivity of Nickel (ε)	0.65
Stefan-Boltzman constant (σ)	1.355×10^{-12} cal/cm^2-sec-°K
Thermal conductivity of Nickel (k)	0.158 cal/sec-cm-°K
Density of Nickel (ρ)	8.9 g/cm^3

TABLE 2.12. Parameters Used in Reference Case

	Plate	Side Rod	Cross Rod
Effective Thickness, cm	0.159	1.078	0.737
Density × thickness (D), g/cm^2	1.41	9.59	6.56
Conductivity × thickness (K), cal/sec-°K	0.025	0.170	0.116
Radiation Parameter (A)	1.762×10^{-12}	3.96×10^{-12}	1.762×10^{-12}
Conductivity from plate to side rod and cross rod	0.025 cal/sec-°K		
Conductivity from side rod to cross rod	0.116 cal/sec-°K		
Time Step	0.1 sec		
Mesh spacing	0.635 cm		
Initial VSR Temperature	20 °C		
Reactor Temperature	1000 °C		

The results of TEMP were compared with an independent calculation[1] which used similar assumptions in a 3-dimensional model with the computer program HEATING.[2] The detailed comparison of results indicated that the two calculations agreed within 25 °F. Since the material properties and radiation heat transfer parameters were chosen independently, this agreement confirms the validity of the 2-dimensional model of the TEMP calculations.

The temperature of one quarter of the plate at the time of largest temperature gradient is shown in a 3-dimensional plot in Figure 2.12. In this plot, the center of the plate is in the upper right hand corner. As indicated in the figure, the

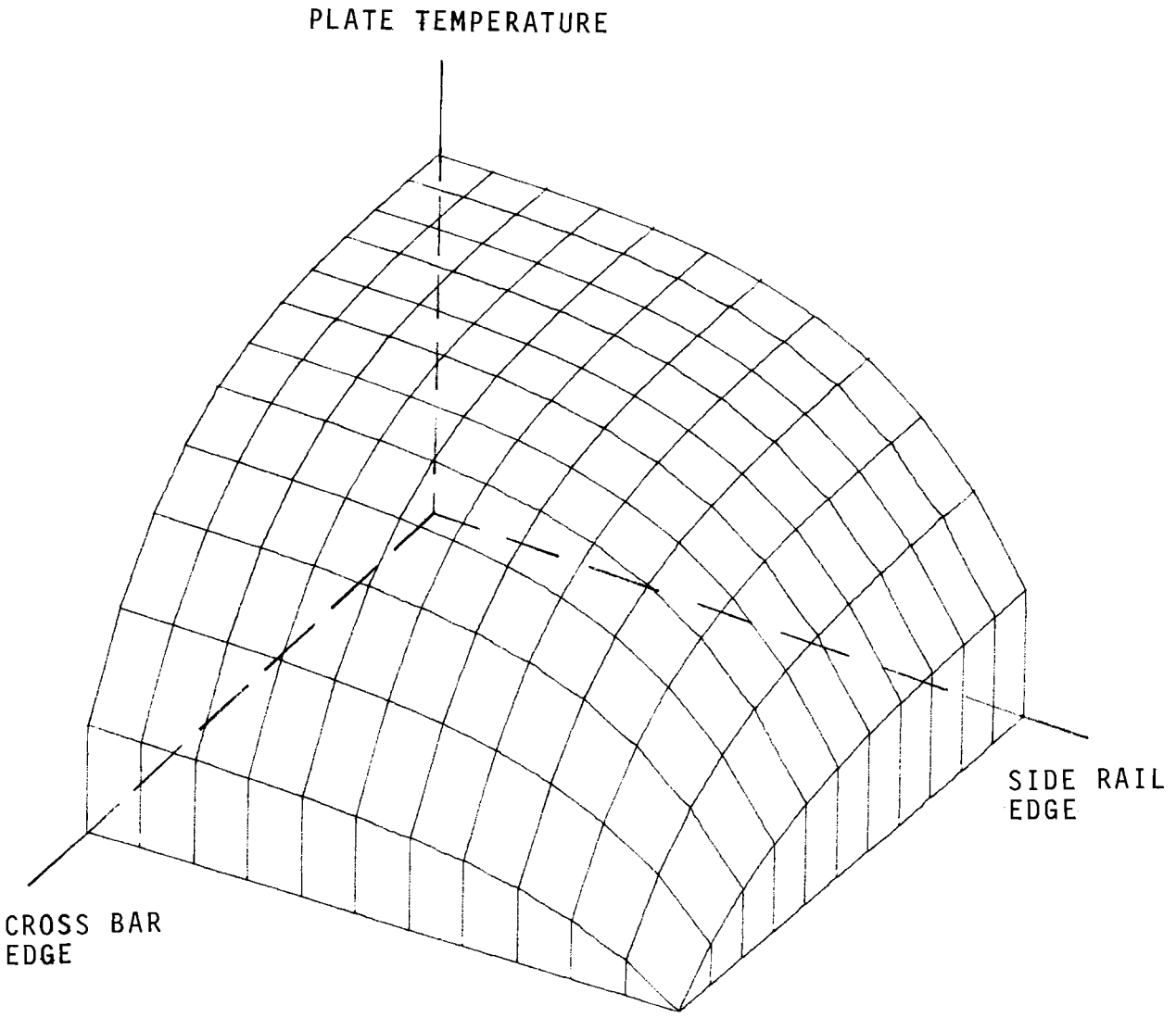

FIGURE 2.12. Three-Dimensional Plot of Temperature of Plate at Time of Maximum Gradient

temperature is relatively constant near the center of the plate and falls off sharply toward the edges. A plot versus time of the temperature of the center of the plate and the temperature difference between the center and edge of the plate is shown in Figure 2.13.

Various cases were run with perturbations on the input parameters. It was observed that changing the emissivity uniformly had very little effect except to change the time scale. However, the maximum gradient can be lessened by decreasing the emissivity of the plate relative to the rods, by increasing the plate thickness, or by lowering the conductivity from the plate to the rods.

The temperature profile as shown in Figure 2.12 formed a basis for a stress calculation.[3] Indicated stresses well beyond those necessary to buckle the plate were computed. The reference calculation therefore can be used as a basis for evaluating possible solutions to the problem. Two categories of possible solutions may be considered: (1) relieving the stresses and (2) minimizing the temperature gradients. Further temperature calculations were made to look at solutions of the second category by adding the TD nickel skin, used in the original VSR design, as a shield for the plates.

TEMP Calculations Assuming Skin Shield

A series of calculations was made to investigate the effect of various thicknesses of skin on one or both sides of the plate. The skin acts as a radiation shield during the time it takes for the skin to heat up and thus the center of the plate remains cool relative to the edges.

Calculations with TEMP utilizing a skin were made by adding a second plate as a skin and taking into account temperature changes in the skin by a formulation similar to that used for the plate. The skin receives radiation on one side

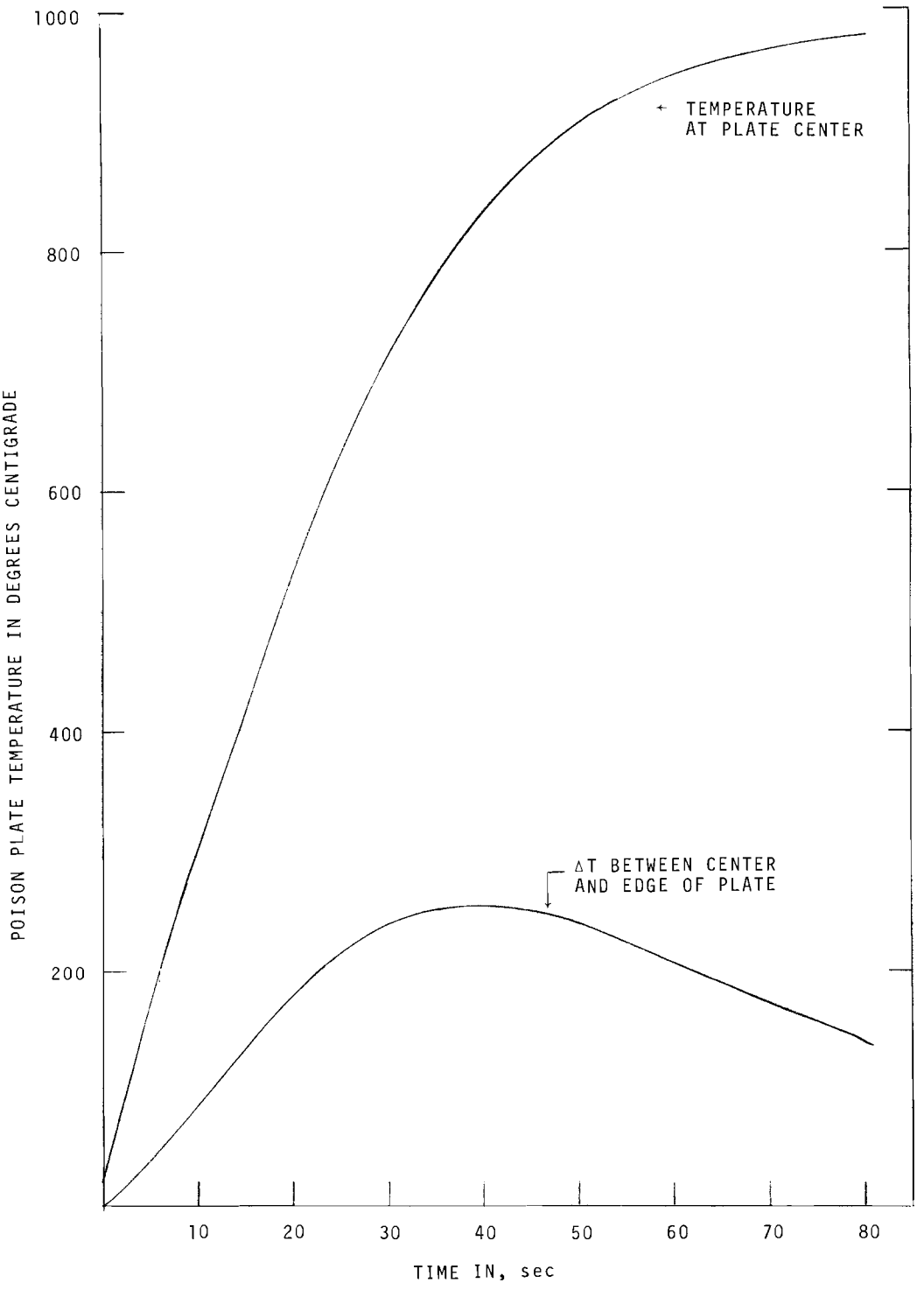

FIGURE 2.13. Temperature Variation in Poison Plate with Time from TEMP Calculations

only from the cavity and radiative transfer between the skin and plate takes place on the other side. Conduction to the plate also can be included, but this was estimated to be a small effect.

Calculations were done with a single skin with radiation directly to the plate on one side. This lowered the maximum center to side temperature difference to about 85 °C (as compared to 256 °C for the unshielded plate) and kept the initial opposite temperature difference small (i.e., the side rods initially heat up faster while heat is built up in the skin). However, unknown temperature gradients might be created by the asymmetry of a skin only on one side so further investigations were limited to the double skin design.

In the double skin case, the worst temperature gradient occurs when the side heats up initially much faster than the center. The magnitude of this gradient depends on the assumptions made, but conservative assumptions about conduction from the skin to plate indicate that this can cause large stresses. This gradient can be lessened by using a thinner skin. In the model used, which assumed some conduction through a rivet to the center point, but no other conduction or convection from the skin to the plate, and half the conduction from the plate to rods used in the reference case, the maximum temperature difference along the x-axis was 109 °C for a 0.030-in. skin, 82 °C for a 0.020-in. skin, and 65 °C for a 0.015 in. thick skin. Making less conservative assumptions would, of course, reduce this difference.

In addition to the above gradient, it was found that with the skins, the cross rods heat up slower than the side rods and the center rapidly gets hotter than this edge. This gradient has the same sign as that in the reference case, and gets worse as a thinner skin is used. However, a stress calculation near

the maximum for this gradient in the 0.015 in. skin case showed stresses that were within tolerable limits.

Conclusions

A TEMP program has been written which can predict temperature gradients created when a vertical safety rod is dropped from room temperature into a hot reactor. The results from this program, when used in a stresss analysis calculation, indicated stresses which accounted for the observed buckling of the present VSR design. In addition, these results can be used in calculations to determine ways of relieving the stresses. Further calculations were carried out which can be used to predict the adequacy of design changes proposed to eliminate the plate buckling. The accuracy of the calculation is limited, however, by assumptions which must be made for the parameters which have not been measured.

References

1. *J. M. Creer. Unpublished Data, Battelle-Northwest. (Personal Communication)*

2. *R. R. Lignori and J. W. Stephenson. "The Heating Programs," Astra vol. 417, p. 510, Astra, Inc, Raleigh, North Carolina. 1961.*

3. *R. M. Selby, Unpublished Data, Battelle-Northwest. (Personal Communication)*

3.0 FAST REACTORS

PCTR MEASUREMENT OF k_∞' FOR A UA1 FAST CORE

D. F. Newman

Introduction

The development of a large fast neutron cavity (FNC) in the Physical Constants Testing Reactor (PCTR)[1] has permitted the application of PCTR methods to fast reactor media. Calculational studies of neutron spectrum buffering requirements for small fast reactor zones in the FNC have identified a broad range of experiments considered feasible in the PCTR/FNC.[2] A small UA1 fast core, containing 13.3 kg ^{235}U was installed in the center of the FNC. Reactivity worths of the central cell and a standard absorber measured in the PCTR were analyzed to determine k_∞' for the fast core.

Analytical Model for the Determination of k_∞'

The analytical model for the determination of k_∞' makes use of the multigroup form for the general perturbation expressions derived by Heineman[3]

$$\chi\Delta\rho = \sum_i \int_S ds\,\phi_i^+ J_i' \tag{1}$$

where

$$\chi = \sum_i \int_{V_o} dV\,\phi_i^+ \phi_i' \tag{2}$$

and S is the surface enclosing the test sample, V_o is the reactor volume exterior to the test sample, and J' is the outward net current at the surface of the test sample.

The multigroup perturbation equation for the reactivity coefficient of the test sample,

$$\chi\Delta\rho^{cell} = V^{cell}\left[\sum_i (\nu\Sigma_f - \Sigma_a)_i \phi_i \phi_i^+\right]^{cell} \quad (3)$$

and for a small copper sample inserted in the test void,

$$-\chi\Delta\rho^{Cu} = V^{Cu}\left[\sum_i \Sigma_{a_i} \phi_i \phi_i^+\right]^{Cu} \quad (4)$$

was obtained from Equation (1).

Eliminating χ from Equations (3) and (4) the ratio of normalized reactivity coefficients can be compared with multigroup calculations:

$$-\frac{\Delta\rho^{cell}}{\Delta\rho^{Cu}} = \frac{V^{cell}\left[\sum_i (\nu\Sigma_f - \Sigma_a)_i \phi_i \phi_i^+\right]^{cell}}{V^{Cu}\left[\sum_i \Sigma_{a_i} \phi_i \phi_i^+\right]^{Cu}}. \quad (5)$$

The infinite medium neutron multiplication factor, k_∞', calculated by various theoretical models is defined as[4]

$$k_\infty' = \frac{\text{Total neutron production}}{\text{Total neutron absorption}} = \frac{\sum_i \nu\Sigma_{f_i} \phi_i'}{\sum_i \Sigma_{a_i} \phi_i'} \quad (6)$$

where ϕ_i' refers to the multigroup equilibrium neutron fluxes in the fundamental mode. The observed neutron multiplication factor for the nonequilibrium spectral environment in the center cell is given by:

$$k_\infty^{cell} = \frac{\sum_i \nu\Sigma_{f_i} \phi_i^{cell}}{\sum_i \Sigma_{a_i} \phi_i^{cell}} = 1 + \frac{\sum_i (\nu\Sigma_f - \Sigma_a)_i \phi_i^{cell}}{\sum_i \Sigma_{a_i} \phi_i^{cell}} \quad (7)$$

for the small fast core installed in the PCTR/FNC. The value of k_∞^{cell} can be inferred from the normalized reactivity coefficients by use of Equation (5),

$$k_\infty^{cell} = 1 + \left(- \frac{\Delta\rho^{cell}}{\Delta\rho^{Cu}} \right) \frac{V^{Cu}}{V^{cell}} \left[\frac{\sum_i (\nu\Sigma_f - \Sigma_a)_i \phi_i}{\sum_i (\nu\Sigma_f - \Sigma_a)_i \phi_i \phi_i^+} \right]^{cell}$$

$$\times \frac{\left[\sum_i \Sigma_{a_i} \phi_i \phi_i^+ \right]^{Cu}}{\left[\sum_i \Sigma_{a_i} \phi_i \right]^{cell}} . \qquad (8)$$

A calculated correction for the nonequilibrium spectral environment was applied to $(k_\infty^{cell} - 1)$ in the determination of k_∞'.

$$k_\infty' = 1 + (k_\infty^{cell} - 1) \left[\frac{\sum_i (\nu\Sigma_f - \Sigma_a)_i \phi_i'}{\sum_i (\nu\Sigma_f - \Sigma_a)_i \phi_i^{cell}} \right.$$

$$\left. \times \frac{\sum_i \Sigma_{a_i} \phi_i^{cell}}{\sum_i \Sigma_{a_i} \phi_i'} \right] . \qquad (9)$$

Combining Equations (8) and (9) we obtain the analytical model for the determination of k_∞' from normalized reactivity coefficients

$$k_\infty' = 1 + \left(- \frac{\Delta\rho^{cell}}{\Delta\rho^{Cu}} \right) \frac{V^{Cu}}{V^{cell}}$$

$$\frac{\left[\sum_i \Sigma_{a_i} \phi_i \phi_i^+\right]^{Cu}}{\left[\sum_i (\nu\Sigma_f - \Sigma_a)_i \phi_i \phi_i^+\right]^{cell}} \left[\frac{\sum_i (\nu\Sigma_f - \Sigma_{a_i}) \phi_i'}{\sum_i \Sigma_{a_i} \phi_i'}\right]. \qquad (10)$$

Evaluation of k_∞' for a UA1 Fast Core

The small fast core zone in the PCTR/FNC shown in Figure 3.1 was composed of aluminum-30 wt% uranium alloy (93% ^{235}U), 23.6 cm diameter by 30.5 cm long. A 0.23 liter UA1 central cell containing 0.231 kg ^{235}U, and a 0.639 kg copper standard absorber were used for reactivity measurements in the center of the fast core. The measured reactivity worths

$$- \frac{\Delta\rho^{cell}}{\Delta\rho^{Cu}} = \frac{1.291 \pm 0.038¢}{0.294 \pm 0.031¢} = 4.387 \pm 0.486$$

were obtained using standard PCTR methods.[5]

A 26 group transport theory calculation in spherical geometry using the PCTR/FNC calculatonal model[1] was made for comparison with experiment, using Equation (5)

$$- \frac{\Delta\rho^{cell}}{\Delta\rho^{Cu}} = \frac{V^{cell}}{V^{Cu}} \frac{\left[\sum_i (\nu\Sigma_f - \Sigma_a)_i \phi_i \phi_i^+\right]^{cell}}{\left[\sum_i \Sigma_{a_i} \phi_i \phi_i^+\right]^{Cu}} = 5.0288.$$

Effective nuclear cross sections were generated from Russian data[6] using the 1 DX[7] code. Direct and adjoint fluxes in the PCTR/FNC were calculated with the DTF-IV[8] transport theory code.

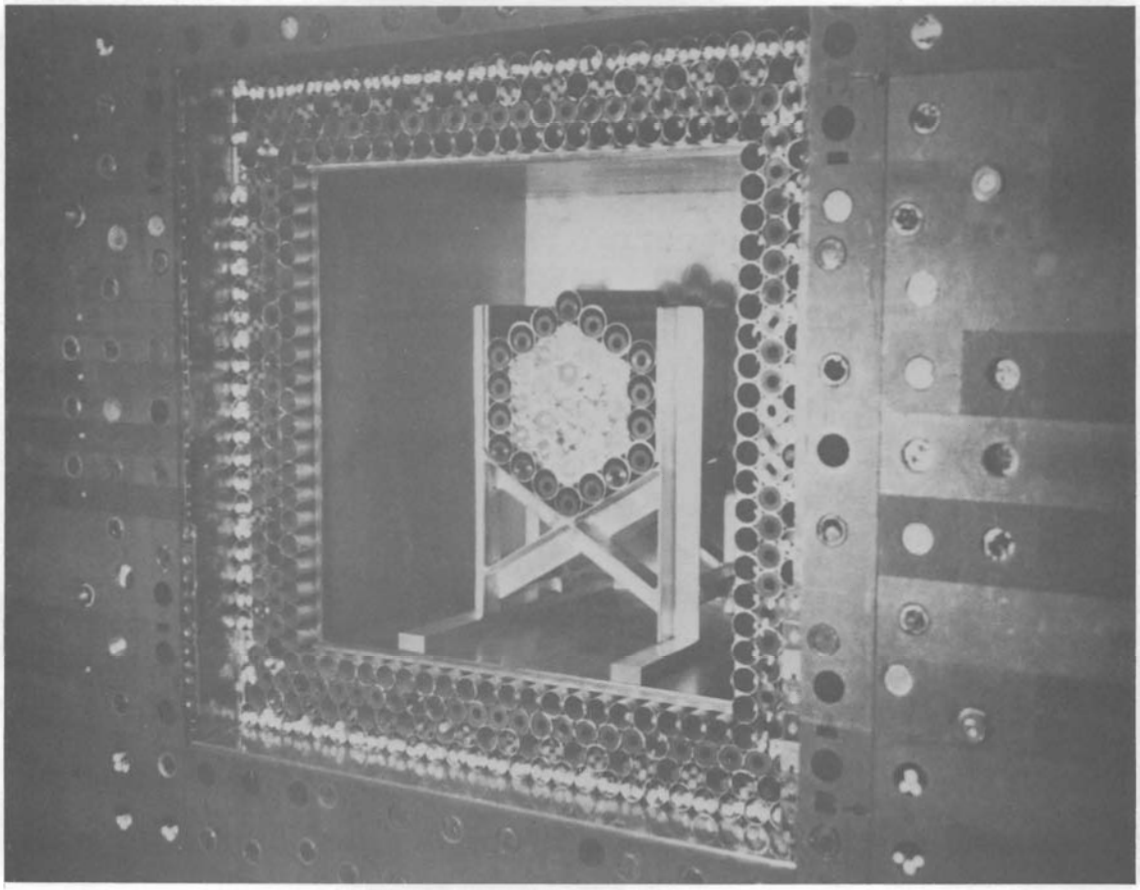

Neg 703343-1

FIGURE 3.1. Aluminum-30 wt% Uranium (93% ^{235}U) Fast Core Installed in the Center of the FNC (Shown with the FNC Front Buffer Removed)

Similar calculations with 1 DX and DTF-IV were made for the UA1 fast core fundamental mode (just critical bare sphere) to correct for the nonequilibrium spectral environment in the PCTR/FNC center cell. Evaluation of k_∞' for the UA1 fast core was made using Equation (10)

$$k_\infty = 1 + \left(\frac{4.387 \pm 0.486}{5.0288}\right)\left(0.98246\right)$$

$$k_\infty' = 1.857 \pm 0.096$$

Calculated values for k_∞' for the UA1 fast core were 1.982 using 1 DX and DTF-IV with 26-group Russian cross section data, and 1.848 using the 68-group EGGNIT[9] code. Comparison of neutron spectra calculated by DTF-IV and EGGNIT, shown in Figure 3.2 indicates that the effect of large scattering resonances in aluminum at 35, 90, and 160 keV, shown in the EGGNIT calculation, is not evident in the Russian cross section data. The difference in k_∞' between the two calculations appears to be due to the differences in the cross section data, shown for comparison in Figure 3.3. The absorption cross section calculated by EGGNIT is larger than the Russian data calculated by 1 DX at neutron energies of interest, as shown in Figure 3.4.

Conclusions

Experiments conducted in the PCTR/FNC with the UA1 fast core have shown that a broad range of fast reactor zoned experiments can be performed in the PCTR. A 10% uncertainty in the reactivity worth of the 0.639 kg copper absorber was the result of using too small a sample. Reactivity worths of both the central cell and standard absorber should be larger than 4¢ to obtain reactivity worth data within a precision of ±1%, one standard deviation. The calculated correction for the nonequilibrium spectral environment in the center of the 13 liter UA1 core was 11.5% of k_∞'-1. This correction could be reduced to 1 or 2% by increasing the fast core volume to 100 liters. The experiment discussed here is a high leakage

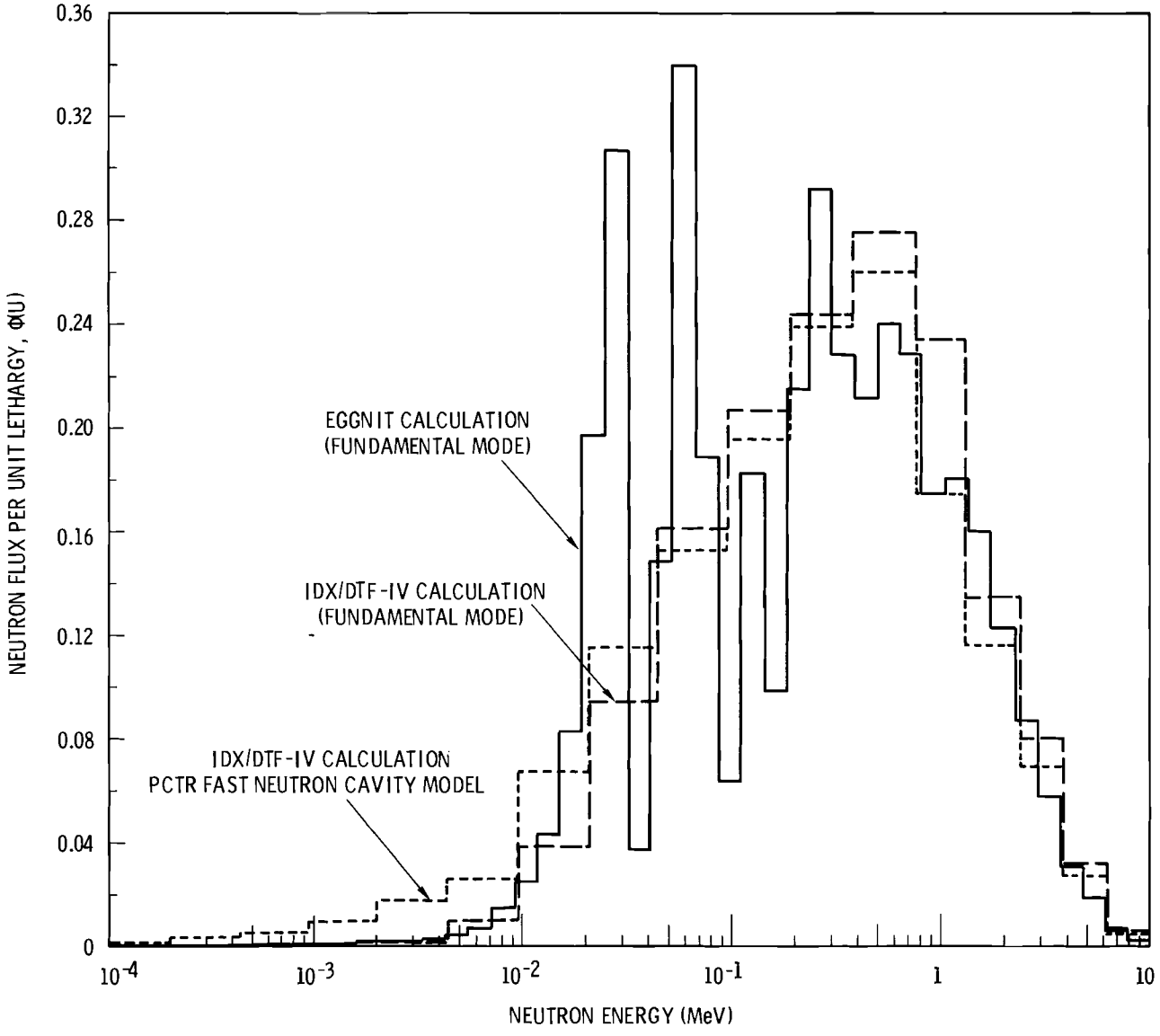

FIGURE 3.2. Calculated Neutron Spectra for an Aluminum-30 wt% Uranium (93% ^{235}U) Fast Core

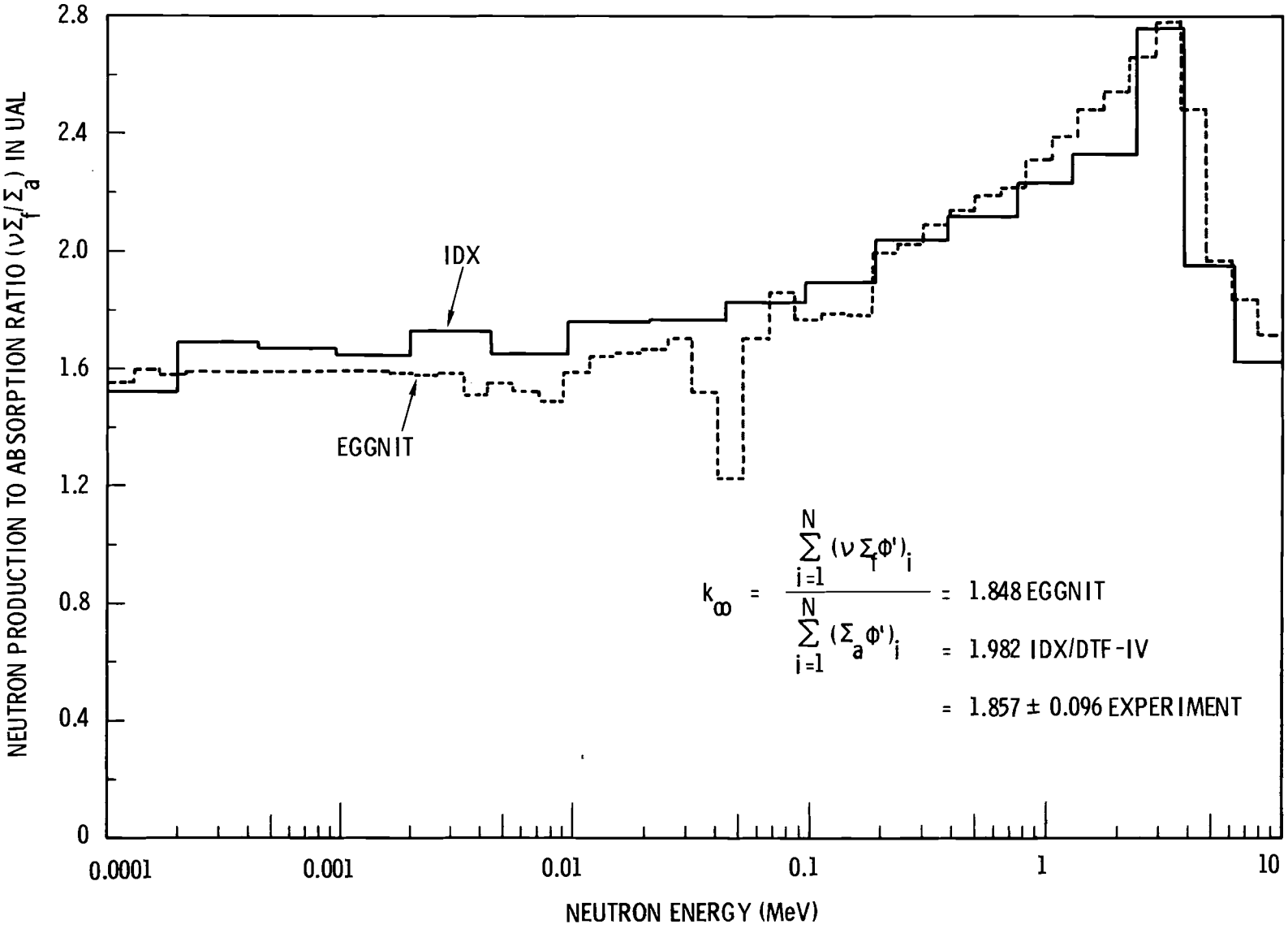

FIGURE 3.3. Comparison of Energy Dependent Neutron Production to Absorption Ratios for the UAL Fast Core

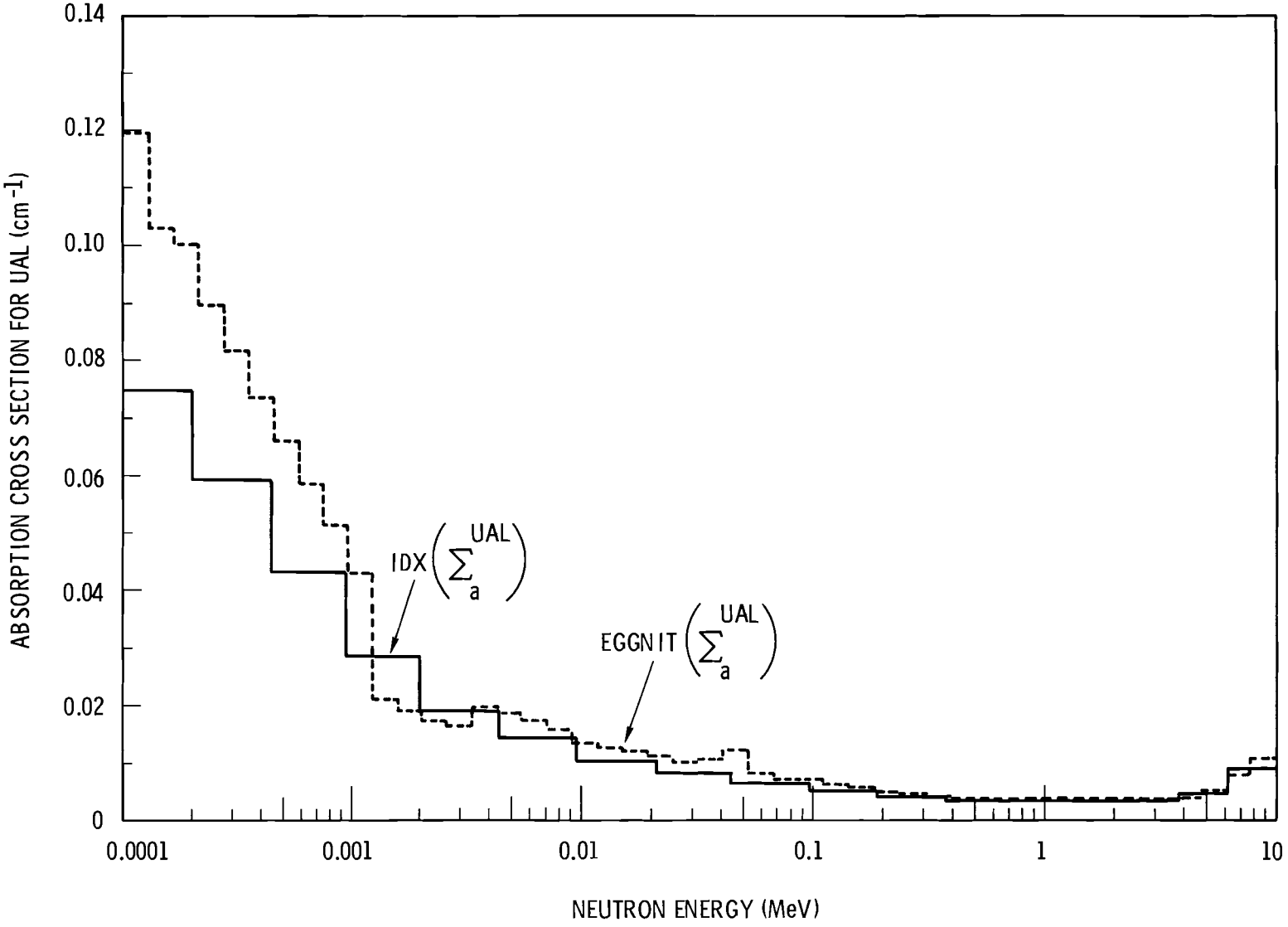

FIGURE 3.4. Comparison of Energy Dependent Neutron Absorption Cross Sections for the UAL Fast Core

test material, and thus, represents a severe test of the method. Very accurate measurements can be made of k_∞ for fast reactor materials having very low leakage[10] (i.e. $k_\infty \approx 1.0$), since the PCTR technique measures $k_\infty - 1$. Fast reactor lattice media typical of large dilute fast breeders are low leakage systems which are expensive to mockup in full size critical experiments. These lattices can be studied in the PCTR/FNC at substantial cost savings for experimental fuel.

References

1. *D. F. Newman. "Fast Reactor Experiments in the PCTR," Reactor Physics Quarterly Report, October, November, December 1969, BNWL-1304, pp. 4.1-4.10, Battelle-Northwest, February, 1970.*

2. *D. F. Newman. "Calculational Comparison of Fast Neutron Cavity and Full Sized Fast Critical Assembly Experiments," Reactor Physics Quarterly Report, January, February, March 1970, BNWL-1381-1, pp. 4.0-4.9, Battelle-Northwest, May 1970.*

3. *R. E. Heineman. "On the Interpretation of Reactivity Measurements of Reactor Media," Proc. ANS, vol. 8, no. 2, pp. 532. 1965.*

4. *E. P. Lippincott, C. R. Richey, and D. D. Lanning. "Definition of the Infinite Neutron Multiplication Factors Measured by the PCTR Poisoned and Unpoisoned Technique," Reactor Physics Quarterly Report, July, August, September, 1969, BNWL-1240, pp. 2.3-2.15, Battelle-Northwest, November 1969.*

5. *R. E. Heineman. Reactivity Measurements on Samples of Multiplying Media, BNWL-SA-263, Battelle-Northwest, November 1965.*

6. *L. P. Abagjan, N. O. Bazazjanc, I. I. Bondarenko, and M. N. Nikolaev. Group Constants for Nuclear Reactor Calculations, Consultants Bureau, New York. 1964.*

7. *R. W. Hardie and W. W. Little, Jr. 1 DX, A One-dimensional Diffusion Code for Generation Effective Nuclear Cross Sections, BNWL-954, Battelle-Northwest. March 1969.*

8. K. D. Lathrop. DFT-IV, A FORTRAN-IV Program for Solving the Multigroup Transport Equation with Anisotropic Scattering, LA-3373, Los Alamos Scientific Laboratory, Los Alamos, New Mexico. 1965.

9. C. R. Richey. EGGNIT: A Multigroup Cross Section Code BNWL-1203, Battelle-Northwest. November 1969.

10. W. N. Fox, R. Richmond, D. J. Skillings, and R. C. Wheller. "The Measurement of ^{239}Pu Capture to Fission Ratios in Fast Reactor Lattices," J. Brit. Nuc. Energy Soc., vol. 6, no. 1, pp. 66. January 1967.

4.0 PUBLICATIONS AND PRESENTATIONS

PUBLICATIONS

J. W. Kutcher and R. I. Smith. Power Tests with the UO_2-2 wt% PuO_2 Batch Core in the PRTR, BNWL-1383. May 1970.*

R. P. Matsen. DBUFIT-I: A Least Squares Analysis Code for Nuclear Burnup Data, BNWL-1396. May 1970.*

James R. Sheff. User's Manual for NOISY1, A Program for Calculation of Space Dependent Spectral Densities in Cubical Reactors, BNWL-1260. May 1970.*

R. W. Hardie and W. W. Little, Jr. 3DB, A Three-Dimensional Diffusion Theory Burnup Code, BNWL-1264. March 1970.*

Alan E. Waltar and William T. Sha. "A New Computational System for Fast Reactor Accident Investigation," Trans. Am. Nucl. Soc., vol. 13, p. 371. 1970.

James R. Sheff. "Stability Analysis of the Fast Test Reactor," Trans. Am. Nucl. Soc., vol. 13, p. 279. 1970.

W. W. Little, R. B. Kidman, R. E. Schenter, L. D. O'Dell, R. W. Hardie, and K. B. Stewart. "Analysis of Critical Experiments Using Version II of the Evaluated Nuclear Data File (ENDF/B)," Trans. Am. Nucl. Soc., vol. 13, p. 304. 1970.

R. A. Bennett, S. L. Engstrom, J. V. Nelson, and W. R. Young. "Statistically Significant Biases in the FTR Neutronics Model," Trans. Am. Nucl. Soc., vol. 13, p. 291. 1970.

S. L. Engstrom, R. A. Bennett, and V. O. Uotinen. "Inverse Multiplication Monitoring of Subcritical Reactivity Changes in FTR," Trans. Am. Nucl. Soc., vol. 13, p. 325. 1970.

R. A. Bennett, S. L. Engstrom, J. V. Nelson, and P. L. Hofmann. "Notes on the Use of the "Engineering Mockup" as a Nuclear Design Tool," Trans. Am. Nucl. Soc., vol., 13, p. 353. 1970.

O. K. Harling. "High-Momentum-Transfer Neutron-Liquid-Helium Scattering, Bose Condensation," Physical Review Letters, vol. 24, p. 1046. 1970.

---

* *BNWL-numbered reports are published by Battelle-Northwest Richland, Washington*

Submitted to Nuclear Science and Engineering

G. D. Seybold. GSSLRN-I: An Automated Least-Squares Computer Code for the Analysis of Photopeak Spectra, BNWL-SA-3234 A.

V. O. Uotinen. The Effect of ^{241}Pu Decay on the Analysis of Plutonium Critical Experiments, BNWL-SA-3157.

V. O. Uotinen, J. H. Lauby, W. P. Stinson, and S. R. Dwivedi. Measured and Calculated $\beta eff/\ell$ for Uniform H_2O Lattices of Al-Pu and UO_2-PuO_2 Fuel Rods, BNWL-SA-3236.

Submitted to Nuclear Applications

S. R. Dwivedi and C. R. Richey. Heterogeneity Correction to Fast-Fission, BNWL-SA-3313.

D. E. Christensen, R. P. Matsen, and R. A. Schneider. Significant Properties of Chemical Reprocessing Plant Accountability Data, BNWL-SA-4036.

Documents in Publication

J. L. Carter. HRG: A Code for Calculating the Slowing-Down Spectrum in the P1 or B1 Approximation, BNWL-1432, to be published.

D. H. Thomsen and T. M. Traver. BMC: The Battelle Monte Carlo Code, BNWL-1433, to be published.

C. L. Bennett and W. L. Purcell. BRT-I: Battelle-Revised-THERMOS-I, BNWL-1434, to be published.

E. C. Davis. Critical Experiments in an MTR-MOCKUP Using Phoenix Fuel, BNWL-SA-4038, to be published.

P. Loizzo, R. Martinelli, N. Pacilio, L. D. Williams, and J. B. Edgar. Experimental and Calculated Results for UO_2 and UO_2-PuO_2 Fueled H_2O-Moderated Loadings, BNWL-1379, to be published.

James R. Sheff. Justification and Specification of an FTR Oscillator, BNWL-1314, to be published.

W. W. Little, R. B. Kidman, L. D. O'Dell, R. W. Hardie, R. E. Schenter, and K. B. Stewart. Analysis of Selected Critical Experiments Using Version II of the Evaluated Nuclear Data File (ENDF/B), BNWL-1348, to be published.

R. W. Hardie and W. W. Little, Jr. User's Manual for the 1DX-2DB-3DB-PERT-V Cord Package, BNWL-1412, to be published.

PRESENTATIONS

D. E. Christensen, R. P. Matsen, R. A. Schneider. "Significant Properties of Chemical Reprocessing Plant Accountability Data," Transactions, ANS, vol. 13, no. 1, p. 48. 1970.

E. P. Lippincott. "Measurement of k_∞ of ThO_2-$^{233}UO_2$ HTGR Lattice," Transactions ANS, vol. 13, no. 1, p. 245. 1970.

J. W. Kutcher, E. C. Davis, C. M. Heeb. "MTR-Phoenix Fuel Critical Experiments and Analysis," Transactions ANS, vol. 13, no. 1, p. 245-246. 1970.

S. L. Engstrom, R. A. Bennett, and V. O. Uotinen. "Inverse Multiplication Monitoring of Subcritical Reactivity Changes in FTR," Transactions, ANS, vol. 13, no. 1, p. 325. 1970.

S. R. Bierman, E. D. Clayton. "Critical Experiments with Homogeneous PuO_2," Transactions ANS, vol. 13, no. 1 p. 379. 1970.

R. G. Clark. "High-Temperature Lattice Test Reactor Operation to 1000 °C," Transactions ANS, vol. 13, no. 1, p. 230. 1970.

Papers Presented at the 16th Annual Meeting of the American Nuclear Society in Los Angeles, California, June 28-July 2, 1970.

S. R. Bierman and E. D. Clayton. Critical Experiments with Homogeneous PuO_2.

R. H. Chow. Analyzer Recycling Between Neutron Bursts Using Gozani's Pulsed-Neutron Technique.

DISTRIBUTION

No. of Copies	
OFFSITE	
2	AEC Chicago Patent Group G. H. Lee
8	AEC Division of Reactor Development and Technology Asst. Dir. for Project Management Chief, Water Project Branch (2) Chief, Gas Cooled Projects Branch Asst. Dir. for Reactor Technology Chief, Reactor Physics Branch (2) Chief, Core Design Branch
1	AEC Division of Nuclear Materials Safeguards H. Werner
1	AEC Division of International Affairs M. B. Kratzer
1	AEC Division of Materials Licensing R. J. Odegaarden
1	AEC Division of Production F. P. Baranowski
2	AEC Division of Reactor Licensing R. E. Ireland P. A. Morris
1	AEC Division of Research G. A. Kolstad
215	AEC Division of Technical Information Extension
1	AEC Savannah River Operations Office R. Thorne
4	Argonne National Laboratory Reactor Physics Constants Center (2) R. Avery P. Gast

No. of Copies	
3	Atomic Energy of Canada Limited M. Duret C. Millar L. Pease
1	Atomic Energy Establishment Dragon Project Winfrith, Dorchester, Dorset, England H. Gutmann
3	Atomic International H. Alter N. Ketzlach Liquid Metals Engineering Center (LMEC)
1	Australian Atomic Energy Commission AAEC Research Establishment Private Mail Bag, Sutherland 2232 N.S.W., Australia Dr. J. L. Symonds Chief, Physics Division
3	Babcock and Wilcox Company H. Jones D. H. Roy W. A. Wittkopf
1	Bechtel Corporation Vernon, California M. Aronchick
1	Bettis Laboratory, Westinghouse Electric Company J. J. Taylor
1	Bhabha Atomic Research Centre Trombay, Bombay-85, India S. R. Dwivedi, Theoretical Physics Section/RED Central Complex Bldg.
3	Brookhaven National Laboratory J. Chernick H. Kouts S. Pearlstein

No. of Copies	
1	California Institute of Technology H. Lurie, Engineering Div.
1	Catholic University of America Dept. of Nuclear Sci. & Eng. Washington, D.C. G. L. Simmons
10	C.E.N. - Saclay Boite Postale 2 Gif-Sur-Yvette (S et 0), France B. LaPonche P. Lecorche G. Vendryes
1	CNEN - Casaccia 00060 - S. Maria Di Galeria Rome, Italy Paolo Loizzo
2	CNEN-Centro Studi-Nucleaire Casaccia, Rome, Italy Ugo Farinelli Augusto Gandini
1	Combusion Engineering, Nuclear Division R. Harding
2	Cornell University, Ithaca, N.Y. R. T. Cuykendall, Eng. Physics M. Nelkin
2	Assoc. C.E.N. Belgo Nucleaire 35 Rue Des Colonies, Belgium H. Bairiot L. Bindler
2	Duke University Durham, N.C. H. W. Newson, Physics Dept. W. J. Seeley, School of Eng.

No. of Copies

6 E. I. du Pont de Nemours & Co., Inc.,
Savannah River Laboratory

H. K. Clark
J. L. Crandall
G. Dessauer
E. J. Hennelly
H. Honeck
J. Suich

10 EURATOM
53, Rue Billiard
Brussels 4, Belgium

A. de Stordeur

1 FFR - AB Afomenergi
Studsvik, Pa NYKOPING
Sweden

Evelyn Sokolowski

4 General Atomic

R. C. Dahlberg
J. M. Neill
H. B. Stewart
G. D. Trimble

3 General Electric Company
Knolls Atomic Power Laboratory

R. Ehrlich
C. Lubitz
K. W. Seeman

4 General Electric Company
San Jose

R. L. Crowther
M. R. Egan
D. L. Fischer
P. Greebler
S. Levy

No. of Copies

1 General Electric Company
Nucleonics Laboratory
H. W. Alter

1 Idaho Nuclear Inc.
R. A. Grimesey

1 Istanbul Technical University
Giimiis, Suyer, Istanbul, Turkey
Director, Nuclear Energy Institute

1 Japan Atomic Energy Research Institute (JAERI)
Tokaimura, Naka-gun, Ibarakiken, Japan
Hjime Sakata

1 Japan Atomic Energy Institute (JPDR-TCA)
Tokaimura, Ibarakiken, Japan
Shojiro Matsuura

1 Kansas State University
Manhattan, Kansas
W. R. Kimel, Nuclear Eng.

1 Kernforschungszentrum Karlsruhe
7500 Karlsruhe, Germany
Professor W. Haefele

1 Los Alamos Scientific Laboratory
G. E. Hansen

1 Manhattan College
Riverdale, New York, N.Y.
Brother Gabriel Kane

3 Massachusetts Institute of Technology
Professor Irving Kaplan
D. D. Lanning
T. J. Thompson

No. of Copies

1 University of Nevada
Reno, Nevada

T. V. Frazier, Physics Dept.

1 University of Notre Dame
Notre Dame, Indiana

E. W. Jerger, Dept. of Mech. Eng.

1 University of Oregon
Eugene, Oregon

J. L. Powell, Physics Dept.

2 University of Tennessee
Knoxville, Tennessee

A. H. Nielsen, Physics Dept.
P. F. Pasqua, Nucl. Eng. Dept.

1 University of Toledo
Toledo, Ohio

J. J. Turin

2 University of Washington
Seattle, Washington

A. L. Babb, Dept. of Nucl. Eng.
K. L. Garlid

1 University of Wisconsin
Madison 6, Wisconsin

M. W. Carbon, Nucl. Eng. Com.

1 U.S. Atomic Energy Commission DNR

A. Radkowsky

1 Virginia Polytechnic Institute
Blacksburg, Virginia

A. Robeson, Physics Dept.

1 Washington State University
Pullman, Washington

J. P. Spielman, Col. of Eng.

No. of Copies	
6	Westinghouse Electric C. A. Anderson R. J. French W. D. Leggett W. L. Orr J. B. Roll J. R. Worden

ONSITE-HANFORD

1	AEC Chicago Patent Group R. K. Sharp (Richland)
2	RDT Assistant Director for Pacific Northwest Programs
2	AEC Richland Operations Office C. L. Robinson (2)
7	Atlantic Richfield Hanford Company S. J. Beard R. D. Carter R. E. Isaacson G. R. Kiel A. E. Smith R. E. Tomlinson ARHCO File
3	Battelle Memorial Institute
2	Computer Sciences Corporation E. Z. Block R. J. Shields
1	Donald W. Douglas Laboratories J. Greenborg
9	Douglas United Nuclear G. F. Bailey C. E. Bowers G. C. Fullmer L. L. Grumme R. O. Gumprecht J. P. Hamric R. H. Meichle R. Nilson DUN File

No. of Copies

17 WADCO Corp.

E. T. Boulette
W. L. Bunch
J. J. Cadwell
E. A. Evans
R. E. Heineman
P. L. Hofmann
R. L. Junkins
W. W. Little
R. E. Peterson
C. A. Rogers
R. E. Schenter
B. Wolfe
WADCO Document Control (5)

93 Battelle-Northwest

F. W. Albaugh
C. A. Bennett
C. L. Bennett
S. R. Bierman
C. L. Brown
S. H. Bush
G. J. Busselman
J. L. Carter
N. E. Carter
D. E. Christensen
R. G. Clark
E. D. Clayton
G. M. Dalen
E. C. Davis
F. G. Dawson
D. R. de Halas
B. H. Duane
J. B. Edgar
G. W. R. Endres
E. A. Eschbach
L. J. Federico
J. R. Fishbaugher
H. A. Fowler
J. J. Fuquay
G. L. Gelhaus
A. G. Gibbs
V. W. Gustafson
C. E. Haines
R. J. Hall
L. E. Hansen
G. E. Hanson

No. of Copies

Battelle-Northwest (contd)

O. K. Harling
W. M. Harris
C. M. Heeb
H. L. Henry
R. J. Hoch
R. H. Holeman
U. P. Jenquin
R. D. Johnson
G. J. Konzek
D. A. Kottwitz
J. W. Kutcher
C. R. Lagergren
J. H. Lauby
B. R. Leonard, Jr.
D. L. Lessor
W. R. Lewis
R. C. Liikala
C. W. Lindenmeier
E. P. Lippincott
R. C. Lloyd
R. P. Matsen
G. C. Moore
D. F. Newman
R. E. Nightingale
T. J. Oakes
D. R. Oden, Jr.
H. M. Parker
R. S. Paul
W. W. Porath
D. L. Prezbindowski
W. L. Purcell
W. A. Reardon
C. R. Richey
W. C. Roesch
J. T. Russell
L. C. Schmid (6)
G. D. Seybold
R. I. Smith
K. B. Stewart
W. P. Stinson
H. J. Svoboda, Jr.
D. H. Thomsen
V. O. Uotinen
A. D. Vaughn
W. P. Walsh
L. D. Williams
N. G. Wittenbrock
W. C. Wolkenhauer
D. C. Worlton
M. G. Zimmerman
Technical Publications (2)
Technical Information (5)